Annu. Rev. Mater. Res. 2002. 32:401–36
doi: 10.1146/annurev.matsci.32.010802.112213

MOLECULAR AND MESOSCALE SIMULATION METHODS FOR POLYMER MATERIALS

Sharon C. Glotzer
Departments of Chemical Engineering and Materials Science and Engineering, University of Michigan, Ann Arbor, Michigan 48109; e-mail: sglotzer@umich.edu

Wolfgang Paul
Department of Physics, Johannes-Gutenberg University, Mainz, Germany; e-mail: Wolfgang.Paul@uni-mainz.de

Key Words modeling, computational materials science, soft materials

■ **Abstract** Polymers offer a wide spectrum of possibilities for materials applications, in part because of the chemical complexity and variability of the constituent molecules, and in part because they can be blended together with other organic as well as inorganic components. The majority of applications of polymeric materials is based on their excellent mechanical properties, which arise from the long-chain nature of the constituents. Microscopically, this means that polymeric materials are able to respond to external forces in a broad frequency range, i.e., with a broad range of relaxation processes. Computer simulation methods are ideally suited to help to understand these processes and the structural properties that lead to them and to further our ability to predict materials properties and behavior. However, the broad range of timescales and underlying structure prohibits any one single simulation method from capturing all of these processes.

This manuscript provides an overview of some of the more popular computational models and methods used today in the field of molecular and mesoscale simulation of polymeric materials, ranging from molecular models and methods that treat electronic degrees of freedom to mesoscopic field theoretic methods.

INTRODUCTION

Polymers are complex macromolecules that display structure ranging from the Å level of the individual backbone bond of a single chain to the scale of the radius of gyration, which can reach tens of nanometers. Polymeric structures in melts, blends and solutions can range from nanometer scales to microns, millimeters and larger. The corresponding time scales of the dynamic processes relevant for different materials properties span an even wider range, from femtoseconds to milliseconds or even seconds or hours in glassy materials or for large scale ordering processes such as phase separation in blends. No single model or simulation

algorithm can span this range of length and time scales. Therefore, molecular and mesoscopic models for polymeric materials range from those including quantum effects and electronic degrees of freedom; to chemically realistic, classical models; to coarse-grained, particle-based mesoscale models that retain only the most essential elements of the polymer system to be simulated; to field-theoretic models that describe the polymer system in terms of density or composition variables. One of the most important problems in computational materials research, which holds particular challenges for polymer materials, is multiscale simulation—the bridging of length and time scales and the linking of computational methods to predict macroscopic properties and behavior from fundamental molecular processes.

Herein we provide an overview of computational models and methods used in the field of molecular and mesoscale simulation of polymeric materials, highlighted by their recent application to important polymer problems. Due to the breadth of the field, this cannot be a comprehensive review. Instead, we focus on a few of the more popular models and methods used in molecular and mesoscale simulation of polymers and, where appropriate, refer the reader to several excellent articles that expand on this topic.

This review is structured as follows. First we present an overview of several different models used to describe polymer systems on particular length and time scales and indicate their typical area of application. We then introduce the computational methods used to simulate these different models. These sections are necessarily cursory and are meant to provide a starting point from which the reader can proceed to the cited literature for more detailed information. We conclude with a discussion of a few selected applications to demonstrate the use of the different levels of modeling and simulation in more detail. The selection of these applications is admittedly influenced by our own research interests, but we endeavor to give a balanced account of what we feel are prominent and important recent developments in the different application areas of molecular and mesoscale simulation of polymeric materials. In the choice of cited literature we again cannot be comprehensive but strive to be balanced and refer the reader to recent review work where we have to be short in our presentation and also to the relevant recent publications that reflect the state of the art in the application of the discussed models and algorithms. The application of computer simulation techniques to polymers has also been the subject of several books over the past ten years (1–4), and a comparative reading of these will provide the interested reader with a more complete perspective on this multifaceted field.

MOLECULAR AND MESOSCALE MODELS FOR POLYMERS

Models with Electronic Degrees of Freedom

At the most basic level of model building, all nuclear and electronic degrees of freedom must be treated quantum mechanically. We therefore consider a

Hamilton-operator

$$\hat{H}(x) = \sum_j \left(-\frac{\hbar^2 \Delta_j}{2m_j} \right) + \sum_k \left(-\frac{\hbar^2 \Delta_k}{2m_e} \right) + V(\{\hat{\mathbf{R}}_j\}, \{\hat{\mathbf{r}}_k\}) \qquad 1.$$

where $\{\hat{\mathbf{R}}_j\}$ and $\{\hat{\mathbf{r}}_k\}$ denote the position operators for the sets of nuclear and electronic degrees of freedom, respectively. The potential V contains all Coulombic interactions. All practical work for condensed phase simulations (5) involves a separation of nuclear and electronic degrees of freedom, e.g., through an adiabatic approximation underlying a Car-Parrinello-type ab initio molecular dynamics (MD) calculation, or through the Born-Oppenheimer approximation leading to a purely electronic Hamiltonian in which the nuclear positions enter only as parameters and not as dynamic degrees of freedom:

$$\sum_k \left(-\frac{\hbar^2 \Delta_k}{2m_e} \right) + V_{ne}(\{\mathbf{R}_j\}, \{\hat{\mathbf{r}}_k\}) + V_{ee}(\{\hat{\mathbf{r}}_k\}). \qquad 2.$$

Here V_{ne} and V_{ee} denote the nucleus-electron and electron-electron interactions, respectively. The consideration of the electronic degrees of freedom is, of course, indispensable for the treatment of optical or electrical properties of polymers (6), but we are not concerned with this area in the following discussion. At the next level of approximation, only nuclear degrees of freedom and their mutual interactions are treated according to classical mechanics.

Chemically Realistic Models of Polymers

Classical atomistic MD and Monte Carlo simulations are based on forcefields parametrizing the energy surface of a given spatial arrangement of the nuclei making up a polymer chain (7). One distinguishes between bonded interactions [bond-length (stretch) potentials, bond-angle (bend) potentials, torsion (twist) potentials and cross-terms] and non-bonded interactions, which in general include Coulomb interactions and dispersion forces, the latter typically parametrized as a Lennard-Jones 12-6 interaction. A typical explicit-atom force field can be written as

$$U(\{\mathbf{R}_i\}) = \sum_j \frac{k_j^l}{2}\left(l_j - l_j^0\right)^2 + \sum_j \frac{k_j^\vartheta}{2}\left(\vartheta_j - \vartheta_j^0\right)^2 + \sum_j \frac{1}{2}\sum_{n=1}^{6} k_{jn}^\phi (1 - \cos(n\phi_j))$$
$$+ \sum_{i,j=1}^{N} \frac{q_i q_j}{R_{ij}} + \sum_{i,j=1}^{N} \varepsilon_{ij} \left[\left(\frac{\sigma_{ij}}{R_{ij}} \right)^{12} - 2 \left(\frac{\sigma_{ij}}{R_{ij}} \right)^{6} \right]. \qquad 3.$$

Here the $\mathbf{R}_i$ denote the positions of the nuclei, $\mathbf{R}_{ij}$ the distance between nuclei i and j, and the q_i their partial charges. The last two sums constitute the non-bonded interactions. In the Lennard-Jones term, the parameters σ_{ij} and ε_{ij} denote the

position and depth, respectively, of the attractive minimum, which depend on the types of the interacting atoms. The first three sums are the bond-length, bond-angle and torsion-angle contributions to the potential energy. The force constants and equilibrium values of bond lengths and bond angles depend on the types of the atoms defining the bond (2-body interaction), bond-angles (3-body interaction) and torsion angles (4-body interaction). The bond-angle term sometimes is not written as a function of the angle but of the cosine of the angle for computational convenience (for small oscillations around the minimum value, both forms are equivalent). Also for computational expedience, the bond-length term, which gives rise to small-amplitude, high-frequency motions, is sometimes replaced by a bond-length constraint, because in a MD simulation, the integration time step must be chosen smaller than the inverse of the largest frequency present in the system. When the above forcefield contains all atom positions, it is called an explicit- or all-atom model. When one is primarily interested in dynamics on picosecond and larger time scales (for instance in polymer melt simulations), it is desirable to neglect the hydrogen atoms in the parametrization of the force-field so that the high-frequency motion of these light atoms can be avoided, and the number of force centers can be significantly reduced. To do this, the hydrogen atoms and the atoms they are attached to are combined to form a so-called united atom, located at or near the position of the atom the hydrogen atoms are attached to and having the combined mass. This procedure constructs a so-called united atom force field. Of course, this can only be a valid description of the polymeric system when there are no partial charges of these groups present and also when hydrogen-bonding effects can be neglected.

Coarse-Grained Molecular and Mesoscopic Models

For many polymeric properties it is not necessary (and in general not computationally feasible) to explicitly take into account all chemical detail. Polymers show a large degree of universality in their static (8) as well as dynamic (9) behavior, and these universal scaling properties as a function of chain length, density, composition, and temperature can be most efficiently studied via coarse-grained molecular models (4). Examples of off-lattice (continuum) models include "pearl-necklace" type models, either of the tangent hard-sphere type (10, 11), where the bond lengths between neighboring pearls along the chain can vary freely within tight limits $b_{\min} \leq b \leq b_{\max}$, or of the bead-spring type (12–15), where neighboring beads are connected by anharmonic springs. More complicated models consisting of ellipsoidal repeat units (16) are also employed. Within the coarse-grained models, one envisions each repeat unit to represent a segment of a realistic chain. Experience from mapping realistic models onto coarse-grained models (17) suggests about four to five carbon-carbon backbone bonds of a typical polymer are represented by a single coarse-grained bond. For this reason, stiffness effects of real polymers are typically not introduced into these coarse-grained models through torsion potentials but rather through bending potentials. Thus one considers a Hamiltonian

of the form

$$H = \sum_i U_b(b_i) + \sum_j U_\theta(\theta_j) + \sum_{kl} U_{nb}(|\mathbf{r}_k - \mathbf{r}_l|), \qquad 4.$$

where i runs over all bonds, j runs over all bond angles, and k, l run over all non-bonded force center pairs in the system. The non-bonded interaction can be either purely hard-core repulsive, soft-core repulsive, or repulsive with an attractive part, such as the Lennard-Jones potential given in the last term of Equation 3.

Such models have been used to study the glass transition (18–22), ordering in block copolymers, phase separation in blends, rubbers, crosslinked polymer networks (23–25), and more. A more computationally demanding type of interaction, such as the long-range Coulomb interaction, is used to model polyelectrolytes (26–28).

Coarse-grained molecular models may also be defined on a lattice. As described below, lattice models may be simulated more efficiently than off-lattice models, allowing the description of phenomena computationally inaccessible to off-lattice simulation methods. Lattice models may describe the polymer as a self-avoiding random walk on some simple lattice, for instance a simple cubic lattice (29) or diamond lattice (30, 31), or be of a type intermediate between these somewhat inflexible lattice models and the continuum case, such as the bond-fluctuation model (32–35). In all these models there is a certain class of allowed bond vectors conforming to the lattice symmetry (6 for the simple cubic lattice, 12 for the diamond lattice, and 108 for the bond-fluctuation model in $d = 3$), and this set of bond vectors defines the set of possible bond lengths and bond angles that can be used as dynamic intramolecular degrees of freedom. The non-bonded interactions in the lattice models are generally realized as contact interactions between neighboring monomers such as, e.g., next neighbors on the simple cubic lattice (36–39), but may also be approximated by discretized Lennard-Jones interactions in the longer-range case (40, 41). Recent work by Panagiotopoulos and Kumar explores the relationship between lattice and off-lattice models for simple systems in order to determine the level of discretization that must be used to achieve off-lattice equilibrium results with a lattice model (42, 43).

Mesoscopic Particle-Based Models of Polymers

In many instances, it is computationally impractical to model polymer systems with a molecular description, even if molecular-level details are represented by coarse-grained expressions, as in bead-spring models of polymers. In such cases, mesoscale simulation methods are used, often with models specific to that particular method. One example is that of dissipative particle dynamics (DPD), a mesoscale simulation technique developed to model Newtonian and non-Newtonian fluids (44–64). In a DPD simulation, described in more detail below, the fluid is modeled as a collection of point particles that represent lumps of fluid containing many molecules. The DPD interaction is considered mesoscopic because the

internal degrees of freedom of the fluid elements are ignored and only their center-of-mass motion is resolved. DPD particles are defined by a mass M_i, position $\boldsymbol{r}_i$, and momentum $\boldsymbol{p}_i$, and interact with each other via a pairwise, two-body, short-ranged force $\boldsymbol{F}^{DPD}$ that is written as the sum of a conservative force $\boldsymbol{F}^C$, dissipative force $\boldsymbol{F}^D$, and random force $\boldsymbol{F}^R$:

$$\mathbf{F}_{ij}^{DPD} = \boldsymbol{F}_{ij}^{C} + \boldsymbol{F}_{ij}^{D} + \boldsymbol{F}_{ij}^{R}. \quad 5.$$

Specific expressions for each force are used and are best discussed in the context of the method; thus we defer further discussion to the methods section below. We note here that extending this model to polymers involves adding a conservative harmonic spring force between adjacent particles in a polymer chain,

$$\mathbf{F}_{ij}^{p} = K(r_{ij} - r_{eq})\mathbf{e}_{ij}, \quad 6.$$

where K is the spring constant, and r_{eq} is the equilibrium spring length. The dissipative particles now become soft beads connected by springs, with each bead representing many atoms.

Mesoscopic Field Theoretic Models of Polymers

Here we briefly describe several field-theoretic models of polymers, each used in a specific mesoscale simulation method to be described in more detail in a subsequent section.

At the simplest mesoscopic level, a polymer system may be modeled by a phenomenological expression for the free energy. For example, the Flory-Huggins or Landau free energies of mixing may be used to model aspects of polymer mixtures (7). In such models, the details of the system are incorporated into, e.g., the Flory χ parameter and the monomer segment mobilities. The time-dependent Ginzburg-Landau or Cahn-Hilliard methods and closely related cell dynamical system methods [see (65) for a review of these methods applied to polymers] utilize these forms to predict the time evolution of mesoscopic structures in multicomponent and/or multiphase polymeric systems such as blends and block copolymers.

Such phenomenological expressions are equivalent to truncated expansions of a more complicated free energy. In the density functional theories used by Fraaije and coworkers (66–70) and by Doi and coworkers (71–73), the full polymer path integral contained in the free energy is retained in a self-consistent mean-field approach in which Gaussian mean-field statistics are assumed. These more detailed but still mean-field models are used in so-called dynamical mean-field density functional theory (DDFT) methods by combining them with coarse-grained time-dependent Ginzburg-Landau (TDGL)-type models for the time evolution of conserved order parameters (66–73).

Most field theoretic treatments of polymers are based upon the Gaussian thread model, where polymers are represented by thread-like, continuous space curves (74). In this model, conformations of non-interacting polymers are given a Gaussian statistical weight with a harmonic stretching energy. Interactions between

monomers on the same or different polymers are typically modeled by pseudopotentials that are often assumed quadratic in the local monomer density. By applying a Hubbard-Stratonovich transformation, the quadratic density interactions can be decoupled, leading to a representation in which different chains are coupled to fluctuating potential fields. Using this approach, field-theoretical models can be easily derived for a variety of multicomponent complex fluids, including polymer solutions, blends, and block copolymers. These models can be then used in several ways (described below) to predict mesoscopic structure in these complex materials. Normally, the integrals contained in these models are approximated within a self-consistent mean-field approach and thus do not contain fluctuations that may be important for many processes. The new field theoretic polymer simulation (FTPS) method recently pioneered by Fredrickson and coworkers (74, 75), and discussed below, allows for the exact solution of these models in order to predict mesoscale structures in polymeric systems beyond what is achieved with mean-field approaches.

Flow and Continuum Mechanics Models of Polymers

For the description of flow of polymeric materials on a processing scale, one must employ a hydrodynamic description and incorporate phenomena occurring on mesoscopic to macroscopic length and time scales. For example, to capture the non-Newtonian properties of polymer flow behavior (76, 77) one can either use special models for the materials stress tensor or obtain it from a molecular simulation using the instantaneous flow properties of the hydrodynamic fields as input. This combined modeling approach has been taken in the CONNFFESSIT project (78, 79). In the area of high-performance materials and devices, polymer composites are finding a widespread application, and the modeling of these materials was until recently done primarily through finite element techniques (80) and are beyond the realm of application of molecular modeling approaches we discuss here. Here commercial finite element packages are typically used, including older software tools such as ABAQUS (www.hks.com) and ANSYS (www.ansys.com), and newer tools such as Palmyra (http://matsim.ch/PalmyraE.html) and OOF (www.ctcms.nist.gov/oof). In the simulation of nanocomposites, in which inorganic materials of nanoscopic dimension are dispersed in a polymeric matrix, efforts to combine models that describe phenomena from molecular through macroscopic levels are underway (81, 82); such efforts in so-called multiscale modeling are described below.

SIMULATION METHODS FOR POLYMERS

Quantum Mechanical Methods

A variety of methods have been developed for the incorporation of quantum effects on the electronic level or the nuclear level, or both. With the advent of the

Car-Parrinello method (83), the class of so-called ab initio methods has undergone an explosive development (5). In this method the nuclei perform thermal motion at some fixed temperature (energy scale), and the electronic degrees of freedom are adiabatically decoupled at a much lower temperature, which keeps the electronic wave function close to a desired state, most often (but not necessarily) the ground state. The forces on the nuclei by the electronic degrees of freedom are determined by the electronic charge density, and the nuclei are propagated using classical MD techniques. Conversely, the nuclei exert forces on the electronic wave functions, which serve as the quantum mechanical degrees of freedom for the electrons.

A complete separation of time scales underlies the Born-Oppenheimer approximation, which leads to a Hamilton operator for the electronic degrees of freedom only. The most common techniques (84) for solving this electronic problem are perturbative techniques such as the Moeller-Plesset perturbation theory, which is an improvement on the self-consistent Hartree approximation or density functional type techniques (85). The Born-Oppenheimer approach is also the basis most often used for the parameterization of force fields for classical MD or MC simulations.

Another type of quantum method is more concerned with the effect of quantum fluctuations on the nuclear coordinates and is based on the path integral approach to the quantum mechanical partition function (86). In this case, the potential energy part of the Hamilton operator can be either given by a fixed force field or determined through a quantum mechanical treatment of the electronic coordinates [ab initio path integral methods (5)]. The path integral can be solved either by MD or MC methods (87, 88).

Classical Molecular Dynamics

MD simulation (89, 90) is a technique for computing equilibrium and transport properties of a classical many-body system, in which the nuclear motion of the molecules can be treated classically, an approximation that is reasonable for many important problems in polymer materials. In MD, molecules move under the action of conservative forces that are additive and symmetric, and derived from intermolecular potentials that are provided as input to the simulation. The rate of change of momentum $\mathbf{p}_i$ of particle i is equal to the sum of the forces acting on it:

$$\dot{\mathbf{p}}_i = \mathbf{F}_i(t) = \sum_{j \neq i} \mathbf{F}_{ij}^C, \qquad 7.$$

where $\boldsymbol{F}_i(t)$ is the force acting on particle i at time t, and $\mathbf{F}_{ij}^C$ is the conservative force acting on particle i due to particle j. The time rate of change of the position $\mathbf{r}_i$ of particle i is given by

$$\dot{\mathbf{r}}_i = \frac{\mathbf{p}_i}{m_i}. \qquad 8.$$

There are several approaches to discretizing and numerically integrating the equations of motion. The most popular is the velocity Verlet method, in which the

position and velocity, $\mathbf{v}_i$, of every particle at time $t + \mathrm{dt}$ are obtained from

$$\mathbf{r}_i(t + dt) = \mathbf{r}_i(t) + \mathbf{v}_i(t)\, dt + \frac{\mathbf{F}_i(t)}{2m_i}(dt)^2$$

$$\mathbf{v}_i(t + dt) = \mathbf{v}_i(t) + \frac{\mathbf{F}_i(t + dt) + \mathbf{F}_i(t)}{2m_i}\, dt. \qquad 9.$$

In its simplest form, the MD method samples states in the microcanonical (NVE) ensemble. Simulations at constant temperature (NVT) and/or pressure (NPT), rather than constant energy, are easily performed by adding an appropriate thermostat and/or barostat (89, 90). It is also straightforward to simulate the non-equilibrium effects of an imposed shear or strain on the system (91, 92).

In an MD simulation, the level of detail the simulation can describe is dictated by the form of the force field, or, equivalently, the interaction potential, which can range from a fully atomistic form to more coarse-grained potentials, as described above. In the former case, the time steps employed in solving the discretized equations of motion for the particles are on the time scale of femtoseconds; in the latter case, the time step may be tens of femtoseconds (in the case of the bead-spring model), or as large as nanoseconds (in the soft force field used in DPD). A useful metric in defining the size of an MD simulation is the number of particle steps performed (i.e., X particles simulated for Y time steps is a simulation of X^*Y particle steps). This metric is more useful than simply the number of particles or the length of the simulation because one must usually trade one to get more of the other. Thus, e.g., there are examples of simulations of a billion atoms simulated for hundreds of time steps, and simulations of a hundred atoms for billions of time steps. One of the largest MD simulations to date is 10^{15} atom steps, achieved for a protein in explicit solvent with long-range interactions (93). For most polymer simulations today, a typical system size may range from 10^{11}–10^{13} particle steps depending on the level of detail (e.g., number of terms, range of forces) included in the force field. For systems where more than one type of interaction is considered (e.g., bonded and non-bonded forces), multiple-time-stepping algorithms such as rRespa (94) have been invented that allow one to accelerate the dynamics by separating and staggering the updates of the different types of forces.

Brownian Dynamics

Brownian dynamics (BD) is a modification of molecular dynamics that is particularly useful when there is a large separation of time scales governing the motion of different components of the system, such as for a polymer in a solvent. There the short time steps required to resolve the fast motion of the solvent molecules means that the evolution of the slower modes of the system, for which a larger time step would have sufficed, will require very long MD runs. However, if the detailed motion of the solvent molecules is not of interest, they may be removed from the simulation and their effects on the polymer represented by dissipative ($-\gamma\mathbf{p}$) and random ($\sigma\xi$(t)) force terms, replacing Newton's equations of motion

by a Langevin equation,

$$\dot{\mathbf{p}}_i = \mathbf{F}_i(t) = \sum_{j \neq i} \mathbf{F}_{ij}^C - \gamma \mathbf{p}_i + \sigma \zeta_i(t), \qquad 10.$$

where γ and σ are constants and depend on the system, and $\zeta(t)$ is a Gaussian random noise term. One consequence of this approximation of the fast degrees of freedom by fluctuating forces is that the energy and momentum are no longer conserved, which implies that the macroscopic behavior of the system will not be hydrodynamic. Additionally, the effect of one solute molecule on another through the flow of solvent molecules is neglected, as is any modification of the interaction between them due to solvent structure. Although there are ways of including these interactions (95), if they are important their explicit simulation by MD should be considered. Brownian dynamics methods for polymer flow problems have been developed by several groups (96–99); Öttinger's book contains further discussion of stochastic polymer simulation methods (100).

Dissipative Particle Dynamics

Dissipative particle dynamics (DPD) is a computational method that allows the simulation of Newtonian and non-Newtonian fluids, including polymer melts and blends, on mesoscopic length and time scales (44–64). Like MD and BD, DPD is a so-called particle-based method, but in a DPD simulation, the elementary unit is not an atom or molecule but a point particle that is meant to represent a fluid element containing many molecules. DPD is in some sense a progression of MD and BD. In this simulation technique, two particles i and j interact via pairwise additive, symmetric 2-body forces that can be written as a sum of conservative, dissipative, and random forces:

$$\mathbf{F}_{ij}^{DPD} = \mathbf{F}_{ij}^C + \mathbf{F}_{ij}^D + \mathbf{F}_{ij}^R. \qquad 11.$$

The total force $\boldsymbol{F}_i(t)$ acting on particle i at time t is

$$\dot{\mathbf{p}}_i = \mathbf{F}_i(t) = \sum_{j \neq i} \mathbf{F}_{ij}^C + \sum_{j \neq i} \mathbf{F}_{ij}^D + \sum_{j \neq i} \mathbf{F}_{ij}^R. \qquad 12.$$

Because the forces are pairwise, momentum is conserved, and thus the macroscopic behavior directly incorporates Navier-Stokes hydrodynamics, instead of having to model its effects through an approximate hydrodynamic tensor as is done in mesoscopic field-theoretic approaches. However, energy is not conserved because of the presence of the dissipative and random force terms. These force terms are similar to those contained in BD, but incorporate the effects of Brownian motion on larger length scales. Moreover, DPD has advantages over BD because the solvent is simulated explicitly in a DPD simulation.

DPD has several advantages over MD. First, because the particles are mesoscopic, hydrodynamic behavior is observed with far fewer particles than required in an MD simulation. Second, the form of the forces used in DPD allow larger

time steps to be taken than in MD. The three-force expressions used to determine the interaction between pairs of particles can be written as (62–64):

$$\begin{aligned} \text{Conservative force:} \quad & \mathbf{F}_{ij}^{C} = \Pi_0 \omega_c(r_{ij})\hat{\mathbf{e}}_{ij} \\ \text{Dissipative force:} \quad & \mathbf{F}_{ij}^{D} = -\gamma \omega_D(r_{ij})(\hat{\mathbf{e}}_{ij} \cdot \mathbf{p}_{ij})\hat{\mathbf{e}}_{ij} \\ \text{Random force:} \quad & \mathbf{F}_{ij}^{R} = \sigma \zeta_{ij} \omega_R(r_{ij})\hat{\mathbf{e}}_{ij}. \end{aligned} \tag{13.}$$

Here $\boldsymbol{r}_{ij} = \boldsymbol{r}_i - \boldsymbol{r}_j$, $r_{ij} = |\boldsymbol{r}_{ij}|$, $\hat{\mathbf{e}}_{ij} = \boldsymbol{r}_{ij}/|r_{ij}|$, $\boldsymbol{p}_{ij} = \boldsymbol{p}_i - \boldsymbol{p}_j$, Π_0 is a constant related to the fluid compressibility, γ is a friction coefficient, σ is a noise amplitude, and ζ_{ij} is a random noise term with zero mean ($\langle \zeta_{ij} \rangle = 0$) and unit variance. The values of ζ_{ij} are uncorrelated for different pairs of particles and for different times such that $\langle \zeta_{ij}(t)\, \zeta_{kl}(t') \rangle = (\delta_{ik}\delta_{jl} + \delta_{il}\delta_{jk})\, \delta(t - t')$. Note that momentum conservation requires $\zeta_{ij} = \zeta_{ji}$.

The form of the interaction potential between particles is governed by the form of the weight functions ω_{C}, ω_{D}, and ω_{R} (62). Whereas in MD the interaction potentials are high-order polynomials of the distance r_{ij} between two particles, in DPD the potentials are softened so as to approximate the effective potential at mesoscopic length scales. The form of the conservative force in particular is chosen in DPD to decrease linearly with increasing r_{ij}. Beyond a certain cut-off separation r_c, the weight functions and thus the forces are all zero. The weight functions are normalized such that (62)

$$\int_V \omega(r)\, d\mathbf{r} = \frac{V}{N}, \tag{14.}$$

where V is the volume of the simulation box and N is the number of particles. In early versions of DPD, the three weight functions were taken to be equal. Español & Warren (101) showed that the system will sample the canonical ensemble and obey the fluctuation-dissipation theorem [in the limit $\delta t \to 0$ (102) if one chooses $\gamma = \frac{\sigma^2}{2k_{\mathrm{B}}T}$ and $\omega_{\mathrm{D}}(r_{ij}) = (\omega_{\mathrm{R}}(r_{ij}))^2$, where k_B is Boltzmann's constant]. The instantaneous temperature of the system is obtained, as in MD,

$$3k_B T = \left\langle \frac{\mathbf{p}_i^2}{m_i} \right\rangle. \tag{15.}$$

In a DPD simulation, the particle momenta may be updated according to the simple discretized Euler equation:

$$\mathbf{p}_i(t + \delta t) = \mathbf{p}_i(t) + \delta t \sum_{j \neq i} \mathbf{F}_{ij}^{C} + \delta t \sum_{j \neq i} \mathbf{F}_{ij}^{D} + \sqrt{\delta t} \sum_{j \neq i} \mathbf{F}_{ij}^{R}. \tag{16.}$$

The $\sqrt{\delta t}$ term arises from the discretization of the stochastic differential equation. The particle positions are then updated according to

$$\mathbf{r}_i(t + \delta t) = \mathbf{r}_i(t) + \frac{\mathbf{p}_i(t + \delta t)}{m_i} \delta t. \tag{17.}$$

However, the velocity Verlet method, which is also used in MD, has been shown to be a preferable integration scheme (52, 103). The units in DPD are dimensionless. The cutoff radius r_c of the particle interaction sets the length scale of the system.

Classical Monte Carlo

The primary task for which the Monte Carlo method was developed is the calculation of thermodynamic averages (104, 105), i.e., high-dimensional configuration space integrals. To sample preferentially the regions of configuration space with large statistical weight, the MC method in its kinetic version numerically solves the following master equation

$$P_{n+1}(x) = P_n(x) + \sum_{x'} W(x' \to x) P_n(x') - \sum_{x} W(x \to x') P_n(x), \qquad 18.$$

where $P_n(x)$ is the probability of finding configuration x at "time" (MC step) n. The transition probabilities from configuration x′ to configuration x, $W(x' \to x)$, are chosen to fulfill the detailed balance condition with the equilibrium probability distribution

$$W(x' \to x) P_{eq}(x') = W(x \to x') P_{eq}(x), \qquad 19.$$

which for most applications is given by the canonical distribution $P_{eq}(x) = \frac{1}{Z} \exp\{-\beta H(x)\}$ where $\beta = \frac{1}{k_B T}$ and the canonical partition function is given by $Z = \sum_x \exp\{-\beta H(x)\}$. In this way, it is guaranteed that in the stationary state of the Markov chain generated by the master equation, all configurations are generated according to their equilibrium statistical weight.

For lattice models, the MC technique is the most common option to define a (pseudo-) kinetics in configuration space (cellular automata type models are also used for this purpose) (106), whereas for off-lattice models it provides an alternative to the MD method. The great advantage of the MC method is the freedom of choice for the transition probabilities, provided detailed balance (or a suitably relaxed condition) (104) is fulfilled. The transition probabilities can thus be optimized to provide for efficient sampling of the configuration space. The flip-side of this is the fact that only for certain classes of transition probabilities are the generated pseudo-kinetics physically reasonable. It is known, for example, that suitably chosen local update rules reproduce the Rouse-like dynamics of short polymer chains (105, 107). The types of moves that are generally explored are the same for lattice and off-lattice models. The local moves either act on intramolecular degrees of freedom (1-bond rotations, 2-bond rotations and 3-bond rotations) (108) or generate random displacements of selected atoms (32–35). A variety of larger-scale MC moves have also been considered: the slithering snake or reptation move (108–111), where one randomly cuts a bond from the end of a chain end and attempts to re-attach it to the other end; configurational bias moves [(112–115); for a review see (116)] where an entire section of a chain is cut and then

randomly regrown; the pivot move (108, 117–119) used for single-chain simulations; concerted rotation moves around several bonds in a chain (120–122); and connectivity altering moves (123, 124), in which a chain end attaches to a monomer on another chain, cutting off one of the two parts of the original chain. Another class of MC methods is defined through altering the thermodynamic ensemble for the simulation from the canonical one to, for example, a semi-grand-canonical ensemble (125–129), which is used for blend simulations and where the identity of a chain is switched to the other species pertaining to a probability given through a fixed chemical potential difference between the two species. Another ensemble used for the determination of phase equilibria is the Gibbs-ensemble (130–132). Here, for example, a polymer liquid and the coexisting vapor phase are simulated concurrently, and exchanges between the two simulation boxes occur according to a fixed chemical potential. A method of increasing importance is that of extended ensemble simulations, in which the physical phase space is artificially extended, for example, in parallel tempering simulations (133–135). Alternatively, one simulates at different strengths of the excluded volume interaction to allow for chain insertion into dense systems (136, 137) or to increase the chain mobility in simulations of dense systems (138, 139). Genetic-type or population control algorithms are often used for single-chain simulations. They involve a sample of representative desired chain configurations that are developed according to given rules followed by a selection process in which the most fit samples are copied and the least fit are pruned. This approach goes back to the pioneering work of Rosenbluth & Rosenbluth and has recently led to simulations of chain lengths of up to several million monomers with the pruned-enriched Rosenbluth method (140).

Lattice Boltzmann Method

Another mesoscale method suited for the efficient treatment of polymer solution dynamics is the Lattice Boltzmann method (141–150). In its application to polymer solution dynamics, the polymer itself is still treated on a coarse-grained molecular level using a bead-spring lattice model, but the solvent molecules are treated on the level of a discretized Boltzmann equation (151). In this way the hydrodynamics of the solvent is correctly captured, and the hydrodynamic interaction between different units on the polymer chain, which is mediated by the hydrodynamic flow generated within the solvent through the motion of the polymer, is present in the simulation without explicit treatment of all solvent molecules. Gonnella et al. showed that by including thermodynamic functions derived from a chosen free energy in a lattice Boltzmann simulation of a fluid it is possible to ensure that the fluid relaxes to a well-defined equlilibrium corresponding to the minimum of the input free energy (148). Other applications of this idea to macromolecular systems include the treatment of the flow of liquid crystalline materials (152, 153). However, the presence of the lattice can introduce spurious dynamics, and one must take care when complex flows near boundaries are of interest.

Time-Dependent Ginzburg-Landau/Cahn-Hilliard Field-Theoretic Mesoscale Simulation Method

A method for simulating phenomena such as phase separation and microphase separation in polymer blends and block copolymers is the time-dependent Ginzburg-Landau (TDGL) method. This method relates the time evolution of one or more spatio-temporal order parameters to derivatives of a free energy that is a functional of these order parameters. The method is based on the Cahn-Hilliard-Cook nonlinear diffusion equation for a binary mixture (154–156), which begins with a continuity equation for each component *i* of the mixture that relates the spatio-temporal concentration (or density) $\phi_i(\boldsymbol{r}, \mathrm{t})$ of that component to the mass current $\mathrm{j}_i(\boldsymbol{r}, \mathrm{t})$, and expresses the conservation of mass in the system. In general, for an *n*-component system, an equation of motion can be written for each component (65):

$$\frac{\partial \phi_i(\mathbf{r}, t)}{\partial t} = -\nabla \cdot j_i(\mathbf{r}, t). \tag{20.}$$

The mass current of component *i* is related to the chemical potential μ_j through

$$j_i(\mathbf{r}, t) = -\sum_{j}^{n-1} M_{ij} \nabla \mu_j + j_T(\mathbf{r}, t), \tag{21.}$$

where M_{ij} is the mobility of component *i* due to *j*, and $\mathrm{j_T}(\boldsymbol{r}, \mathrm{t})$ is the mass current arising from thermal noise. The chemical potential μ_j is related thermodynamically to the free energy functional $\mathrm{F}\{\phi_\mathrm{i}(\boldsymbol{r}, \mathrm{t}), \phi_\mathrm{j}(\boldsymbol{r}, \mathrm{t}), \ldots, \phi_{\mathrm{n}-1}(\boldsymbol{r}, \mathrm{t})\}$ by $\mu_j = \delta F / \delta \phi_j$ and the constraint $\phi_\mathrm{i} + \phi_\mathrm{j} + \cdots + \phi_\mathrm{n} = 1$. For an incompressible binary polymer blend, there results only one equation of motion:

$$\frac{\partial \phi(\mathbf{r}, t)}{\partial t} = \nabla \cdot M \nabla \frac{\delta F[\phi(\mathbf{r}, t)]}{\delta \phi(\mathbf{r}, t)} + \eta(\mathbf{r}, t). \tag{22.}$$

Here $\eta(\mathbf{r}, t)$ is a thermal noise term with zero mean and a variance given by the fluctuation-dissipation theorem: $\langle \eta(\mathbf{r}, t)\, \eta(\mathbf{r}', t') \rangle = -2 M k_B T \nabla^2 \delta(\mathbf{r} - \mathbf{r}')\, \delta(t - t')$. In this general form of the equation of motion, any form for the free energy *F* may be used, and the mobility *M* may depend on the order parameter ϕ. For a binary polymer blend, one typically takes

$$\frac{F[\phi(\mathbf{r})]}{k_B T} = \int d\mathbf{r} \left[\frac{f_{FH}[\phi(\mathbf{r})]}{k_B T} + \kappa(\phi)\, |\nabla \phi(\mathbf{r})|^2 \right], \tag{23.}$$

where $\mathrm{f_{FH}}(\phi)$ is the Flory-Huggins (FH) free energy of mixing,

$$\frac{f_{FH}(\phi)}{k_B T} = \frac{\phi}{N_A} \ln \phi + \frac{(1 - \phi)}{N_B} \ln(1 - \phi) + \chi \phi (1 - \phi). \tag{24.}$$

Here χ is the enthalpic interaction parameter between the two polymer components.

The FH model has a critical point at $\phi_c = N_B^{1/2}/(N_A^{1/2}+N_B^{1/2})$ and $\chi_c = (N_A^{1/2}+N_B^{1/2})^2/2N_AN_B$ such that the system is miscible for $\chi < \chi_c$ and immiscible for $\chi > \chi_c$ at the critical concentration. For symmetric blends, in which $N_A = N_B = N$, $\phi_c = 1/2$ and $\chi_c = 2/N$. Two limiting cases of a phase-separated blend are often considered: (*a*) the weak segregation limit (WSL), in which $\chi N \approx 2$ so that the blend is close to the critical point and (*b*) the strong segregation limit (SSL) in which $\chi N \gg 2$ so that the blend is strongly immiscible.

The square gradient term describes the energy necessary to create an interface between homogeneous domains. In the original theory, the coefficient κ of the square-gradient term is enthalpic, independent of the local value of the order parameter, and given by $\chi\lambda^2$, where λ is the effective interaction distance between molecules. For incompressible polymeric systems, one often adds an entropic term to κ:

$$\kappa(\phi) = \frac{1}{36}\left[\frac{l_A^2}{\phi(\mathbf{r})} + \frac{l_B^2}{[1-\phi(\mathbf{r})]}\right], \tag{25.}$$

where l_i is the Kuhn length of species *i*. The combined enthalpic and entropic expression is consistent with the random phase approximation result for the inverse structure factor of an incompressible blend,

$$S^{-1}(q) = \frac{1}{N_A\phi D_A(q^2R_A^2)} + \frac{1}{N_B(1-\phi)D_B(q^2R_B^2)} - 2\chi, \tag{26.}$$

where R_i^2 is the average square radius of gyration of species *i*, and the Debye function $\mathrm{D(x)} = 2(\mathrm{x}-1+\mathrm{e}^{-\mathrm{x}})/\mathrm{x}^2$. In the WSL, the interfacial width is much larger than the chain dimensions, so that $\mathrm{q}^2\mathrm{R}^2 \ll 1$, and the Debye function may be approximated by $\mathrm{D}^{-1}(\mathrm{x}) = 1 + \mathrm{x}/3 + \mathrm{O}(\mathrm{x}^2)$. The square gradient coefficient $\kappa(\phi)$ is then obtained from the coefficient of the q^2 term in the Taylor expansion of the inverse structure factor, which is related to the free energy functional as $\mathrm{q} \to 0$ by

$$\lim_{q\to 0} S^{-1}(q) = \frac{1}{k_BT}\frac{\delta^2 F}{\delta\phi^2}. \tag{27.}$$

Because χ is typically small, the entropic contribution to κ dominates in most cases. For example, for the symmetric polybutadiene blend studied by Bates and coworkers (157), a typical quench temperature of 35°C corresponds to $\chi = 0.00083$; the entropic part of κ is at least two orders of magnitude larger. In practice, it is observed that including a ϕ-dependent κ increases the width of the interfacial region, but does not affect the domain growth laws.

Note that for small molecules ($N = 1$), the free energy of mixing may be approximated via a Taylor expansion around the critical point by the Landau form,

$$\frac{f(\psi)}{k_BT} = r\psi^2 + g\psi^4, \tag{28.}$$

where $\mathrm{r} = (\chi_\mathrm{c} - \chi)/4$, $\mathrm{g} = 1/12$, and $\psi = 2\phi - 1$. The Ginzburg-Landau free

energy functional is then the CH functional with the Landau form of the bulk free energy:

$$\frac{F_{GL}[\psi(\mathbf{r})]}{k_B T} = \int d\mathbf{r}[r\psi^2 + g\psi^4 + \kappa' |\nabla\psi(\mathbf{r})|^2], \qquad 29.$$

where $\kappa' = \chi\lambda^2/4$.

This method was first proposed by Cahn and Hilliard for metallic systems and is used in other fields to model, e.g., the development of dendrites in metallic alloys during solidification. Unlike in metallic systems, however, polymeric systems exhibit viscoelastic and hydrodynamic behavior that can have a strong influence on the mesoscale structures that develop. Both behaviors have been incorporated into TDGL approaches by including additional tensorial equations of motion that couple to the equations for the primary order parameter(s) (158–162). The resulting set of equations are necessarily complicated and can be most efficiently solved using a parallel computing architecture and a spatial decomposition scheme because the update of an equation at a particular grid point requires only the information from the previous time at that grid point and at the nearest neighbor grid points. The simplest form of the TDGL model described here may be solved by an explicit first-order Euler numerical integration scheme, but it is more efficiently solved by the combination implicit-explicit method developed by D. Eyre (unpublished work).

A simplification of the "bare" TDGL method is provided by the cell dynamical system method (163–166), in which the discretized TDGL equation is replaced by a simpler discretized equation in which the Laplacian term is replaced by its isotropic discretized counterpart, $f(\phi) = A\tanh\phi$, and the free energy functional corresponds in the continuum limit to

$$\frac{F_{CDS}[\phi(\mathbf{r})]}{k_B T} = \int d\mathbf{r}\left[-A\ln(\cosh\phi) + \frac{1}{2}\phi^2 + \frac{D}{2}|\nabla\phi(\mathbf{r})|^2\right]. \qquad 30.$$

This model reproduces the growth kinetics (i.e., scaling function and scaling exponents) of the TDGL model, demonstrating that such quantities are insensitive to the precise form of the double-well potential of the bulk free energy term.

Dynamical Density Functional Theory Methods

A similar method used to model complex dynamical behavior of polymeric systems is based on the dynamic density functional theory (DDFT). One implementation of this approach developed by Fraaije and coworkers forms the basis for the software package Mesodyn™ from Accelrys (www.accelrys.com) (66–70, 167–182). DDFT models the behavior of polymeric fluids by combining Gaussian mean-field statistics with a TDGL model for the time evolution of conserved order parameters. However, in contrast to traditional phenomenological free-energy expansion methods employed in the TDGL approach, the free energy is not truncated, and instead retains the full polymer path integral numerically. At the expense of a more

challenging computation, this allows detailed information about a specific polymer system beyond simply the Flory-Huggins χ parameter and mobilities to be included in the simulation. In addition, viscoelasticity, which is not included in TDGL approaches using only FH or Landau free energies, is included at the level of the Gaussian chains. A similar DDFT approach has been developed by Doi (71–73) and forms the basis for his new software tool SUSHI (Simulation Utilities for Soft and Hard Interfaces), one of a suite of molecular and mesoscale modeling tools developed at Nagoya University for the simulation of polymer materials (http://octa.jp).

TDGL and DDFT methods have been successfully used to simulate spinodal decomposition in binary and ternary blends and block copolymers, both in bulk and near surfaces. They have also been used to model the influence of filler particles (183–191) and chemical reactions (192–196) on phase separation behavior. By treating the polymeric system with a field description that incorporates molecular details implicitly, rather than with an explicit atomistic description, these methods are able to simulate phenomena on length and time scales presently inaccessible to traditional MD methods. The DPD method discussed above, which can access the same time and length scales, has an advantage over TDGL and DDFT methods in that the equations to be solved are far simpler, and hydrodynamic behavior results naturally without the need for additional fields and equations.

Field-Theoretic Polymer Simulation Method

The field theoretical models arising from the Gaussian Thread Model described above involve complicated integrals, which may be approximated using various techniques. For block copolymer melts, a mean-field or saddle point approximation (self-consistent mean-field theory) is typically employed as a numerical strategy (197). In a new approach pioneered by Fredrickson and coworkers (74, 75), direct numerical sampling of the relevant functional integrals is achieved via various techniques (including steepest descent methods and complex Langevin dynamics) to obtain exact numerical results.

The field-theoretic polymer simulation (FTPS) formalism is an exact re-expression of the microscopic theory in terms of complex chemical potential fields. Embedded in the expression for the energy functional is the exact solution of the partition function of one polymer in the instantaneous field environment. This implies, for example, that if the fields are inhomogeneous on a scale comparable to the radius of gyration, the method will capture the chain stretching of a diblock copolymer near the order-disorder transition. The FTPS method may prove to be superior for generating equilibrium mesophases in a variety of polymer systems; already, it has been successfully applied to polymer solutions, multicomponent polymer melts, and diblock copolymers. In particular, because it is exact, it includes fluctuations not included in mean-field approximations, which are important for many processes. Note that because the dynamical trajectories generated in the FTPS approach do not conserve momentum, the method fails to capture hydrodynamic

behavior. Also, the FTPS method is restricted to soft repulsive potentials, such as those used in DPD, and thus the method will not describe reptation dynamics in dense melts, which requires entanglement constraints (74).

Multiscale Simulations

A goal of computational materials science is the rapid and accurate prediction of new materials and new properties and features of materials. The methods described in this review have made it possible to do that to some extent. To truly link macroscopic or even mesoscopic phenomena to a detailed molecular description, particularly in the absence of a quantitative, molecular-based theory, will require the bridging of models and simulation techniques across the broad range of length and time scales between the molecular and macroscopic worlds. This type of simulation approach is known as multiscale simulation, a topic that is now receiving a great deal of attention.

One of the first breakthrough examples of multiscale modeling of materials is the linking of quantum and classical molecular methods with continuum methods to study crack propagation in silicon (199). Here tight-binding MD was carried out near the crack tip, classical MD was employed farther away, and finite element calculations were performed far enough from the crack that a continuum approximation was valid. By developing clever schemes to link the three methods together both spatially and temporally, the entire hybrid simulation could be carried out with all three techniques operating simultaneously in the appropriate areas.

Multiscale simulation poses, in some sense, greater challenges for polymer materials than for metallic and ceramic materials due to the larger range of length and time scales that characterize polymers. Although nothing comparable to the silicon simulations has yet been reported, work is being done in that direction by many groups. For example, Doi has developed a suite of state-of-the-art simulation tools that model polymers at the molecular and mesoscale method. Although each tool performs calculations using only one method, the output from one method can be used directly as input for another, allowing an off-line bridging of length and time scales. To achieve what he and others refer to as "seamless zooming"—the ability to spawn higher resolution simulations using more detailed methods where needed—will require additional theoretical and computational advances. Along similar lines, off-line multiscale simulations of nanofilled polymers using coarse-grained molecular dynamics, mesoscopic TDGL, and macroscopic continuum finite element techniques have been carried out (81, 82). Significant advances in uniquely mapping atomistic models of polymers onto coarse-grained models have been made in recent years, in some cases providing nearly exact quantitative agreement between the two models for certain quantities, but these mappings, too, are performed off-line, and the various methods are not linked within a single simulation (17, 200). Future work in multiscale modeling and simulation of polymers will require improved coarse-graining procedures, in particular reverse-mapping procedures, and the linking of multiple methods to span from the quantum mechanical domain (few atoms) to the molecular domain (many atoms) to the

mesoscopic domain (many monomers/many chains) to the macroscopic domain (many domains or structures) (200).

APPLICATIONS

In this section, we present examples of the application of several molecular and mesoscale simulation methods to polymers.

Quantum Mechanical Simulations

Three applications of simulation methods to polymer material problems that take into account quantum fluctuations or treat the electronic degrees of freedom explicitly are described here. The first one is an application of the Car-Parrinello technique to the simulation of the Ziegler-Natta heterogeneous catalysis of polyolefins on a $MgCl_2$ substrate. The unique property of the ab initio methods is the ability to describe chemical reactions on a detailed electronic level. Boero et al. (201) showed which of the molecular forms of the catalyst (a titanium-chloride molecule) discussed in the literature is stable in the catalytic reaction and which of the vicinal surfaces of the magnesium-chloride crystal carry the reaction. The state-of-the-art application of this method produced a singular contribution to the understanding of a chemical process of significant industrial importance.

A different approach is needed when one wants to understand the importance of quantum fluctuations of the nuclear coordinates on the properties of polymer crystals. Martonak et al. (202) performed comparative constant pressure classical MC simulations and constant pressure path-integral MC simulations of alkane crystals employing an explicit atom classical force field for polyethylene (203). The lattice parameters of the crystalline unit cell in both simulations were within 1% of the experimentally known values. However, the fluctuations of the atoms around their equilibrium positions and of the intramolecular degrees of freedom, such as bond lengths, bond angles, and torsion angles, did not go to zero with decreasing temperature in the quantum simulation as they would in a classical simulation, but rather leveled off at their quantum value. This has an influence on the mechanical stiffness of the crystal at low temperatures as is most clearly seen in the behavior of the elastic constant c_{33} connected with the stiffness in the chain direction (see Figure 1). The quantum fluctuations of the torsion angles led to a softening of this elastic constant with respect to the value obtained in the classical simulation that is observable up to temperatures of about 200 K. As for the simulations of the molten state that are discussed below, polyethylene or alkanes have served as the fruitfly for the simulations of polymer crystals (204, 205).

Born-Oppenheimer-based calculations of the electronic ground state energy for a given conformation of a molecule provide a link between quantum simulations and classical MD and MC simulations when they are combined with forcefield parametrization techniques. For the determination of force-field parameters such as equilibrium bond lengths and angles and torsional isomeric states, there is experimental information available, for instance, from X-ray crystallography or

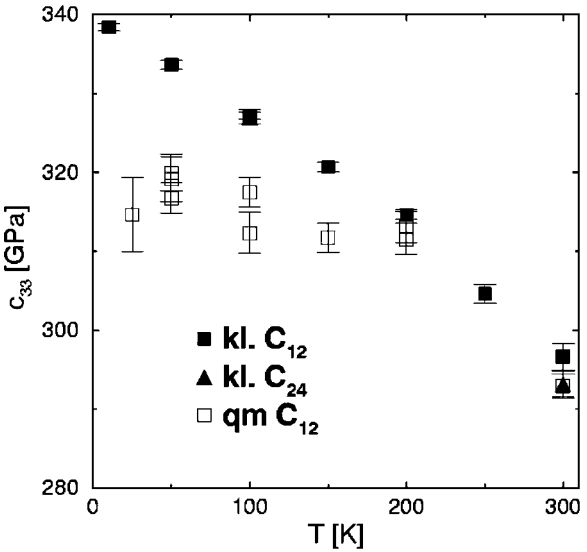

Figure 1 Elastic constant along the *z*-axes for an alkane crystal for chains of length 12 and 24. The quantum fluctuations lead to a softening of the crystal at low temperatures compared with the classical result. From (202).

gas phase spectroscopy. However, these techniques provide no information on the barriers between isomeric states. In polymer liquids, relaxation processes are coupled to the torsional dynamics and therefore to the rate at which these barriers are traversed. Transition state theory tells us that these rates are exponentially sensitive to the height of the barrier above the isomeric states.

For an accurate quantitative simulation of the dynamics of polymeric liquids employing chemically realistic force-fields, it is therefore indispensable to have a very accurate determination of the complete form of the torsion potential. Although the use of density functional techniques to perform this task is growing (84), the generally employed methods (206–210) are perturbative calculations of the Moeller-Plesset type. These calculations are performed on model compounds representing segments of the polymer under study, which have to be large enough to capture correlations between intramolecular degrees of freedom, especially adjacent torsion angles. One of these compounds (*cis*-pentene) used for the parametrization of a force field for 1,4–polybutadiene (210) is shown in Figure 2. For the calculation of the potential for rotations around the α-bond adjacent to the double bond, the molecule is first set up in an optimized geometry for the other degrees of freedom. Then this torsion angle is set to a fixed value, and the electronic ground state is determined allowing the other degrees of freedom to relax. Note that in this way, the potential energy as a function of dihedral angle is calculated as a difference of two large numbers: $U(\phi) = E(\phi) - E_{\min}(\phi)$. Within these calculations the barrier heights can be determined to within an error of about 0.2 kcal/mol or

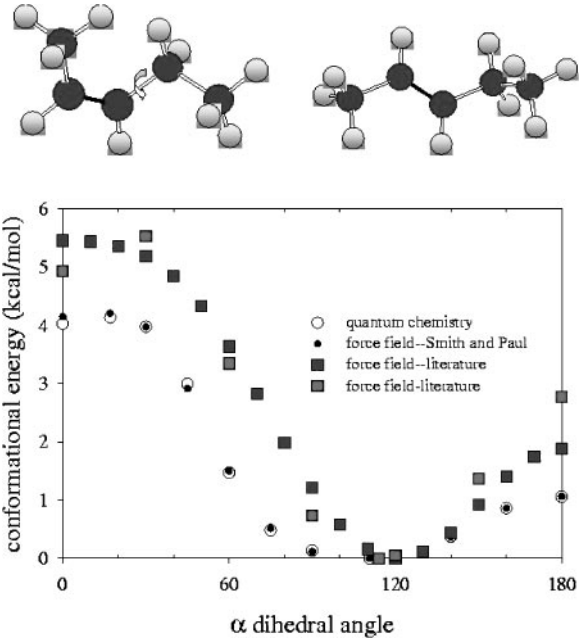

Figure 2 Dihedral potential for rotations around the alkyl bond in *cis*-pentene. The recent quantum chemistry results differ significantly from the literature force-fields. From (206).

100 K, which corresponds to an error in the energy calculations in the sub 1% range. However, typical polymer liquid simulations are performed in the temperature range of 200 to 400 K so that the barrier transition rates $W \propto \exp\{-\frac{\Delta E}{k_B T}\}$ are still sensitive to this uncertainty. A direct quantitative comparison with nuclear magnetic resonance (NMR) experiments (211) can be used for a final fine-tuning of the potential within the quantum chemical uncertainties. Accurate force fields, obtained through a judicious combination of experimental data and quantum chemical calculations, are indispensable for a quantitatively valid modeling of polymer materials properties using chemically realistic models (described below). There are several standard force fields available commercially that usually are not optimized for specific polymers and therefore, in general, cannot be expected to yield a high level of quantitative agreement with experiment across a range of temperature, density, and pressure.

Chemically Realistic Modeling of Structural and Thermophysical Properties

Here we focus mainly on applications of modern advanced MC techniques to determine thermophysical properties of polymer solutions and melts employing chemically realistic force fields. One such application is the combination of

configurational bias moves and Gibbs-ensemble simulation to determine the liquid-vapor coexistence curve of alkanes (212–214). The liquid-vapor coexistence curve of alkanes is experimentally inaccessible for chain lengths greater than about C_{12} because the critical region of the phase diagrams for these chains lies at temperatures where the compounds are thermally unstable. Gibbs ensemble simulations are especially designed to treat this problem by simulating the coexisting phases concurrently in two different simulation boxes. By allowing for volume and particle exchanges between the two boxes at fixed temperatures, the simulated boxes are driven toward coexistence and the binodal line can be traced. Siepmann et al. (212) determined the phase diagram of alkanes up to C_{48} and showed that the MC results were in good agreement with experimental data. To achieve this agreement, however, they had to modify existing force fields for alkanes from the literature. None of the literature force fields employed non-bonded interaction parameters suited to reproduce the experimental phase diagrams. In this way they also showed that the determination of phase diagrams is a highly sensitive means of testing the parameters for the dispersion-type interactions (they employed the Lennard-Jones interaction potential), which are so far not obtainable through quantum chemical calculations. Furthermore, they were able to resolve a disagreement between two existing sets of experimental data as to the dependence of the critical density on chain length and showed that it actually decreases for chains longer than about 10 repeat units. These scaling type properties of the critical behavior $[\rho_c(N), T_c(N)]$ were also studied extensively by MC simulations of coarse-grained models (215, 216). Kumar & Weinhold (217) performed Gibbs ensemble simulations of a bead-spring type model to show that the standard Flory-Huggins theory of polymer phase behavior is not sufficient.

Another important development in the application of advanced MC methods to polymer materials is the use of sophisticated MC moves to equilibrate atomistic models of polymer melts. The quantitative understanding of the dynamic behavior of the molten state of specific polymers is of great importance for polymer-processing industries. Although these MC techniques are not directly suited to study these dynamic properties, they furnish the necessary starting point for dynamical studies using MD techniques or dynamic MC techniques. It is notoriously difficult in a computer simulation to equilibrate even simple coarse-grained models of polymer melts, let alone a chemically realistic one (218). On the other hand, starting from a well-equilibrated system for the study of relaxation behavior is indispensable if quantitatively correct results are desired. The typical relaxation time scales that one obtains at a low-temperature following a quench can differ by an order of magnitude from the real behavior [see (219) for an analysis using a coarse-grained model]. One must bear in mind that the typical quench rates employed in computer simulations are roughly 10 orders of magnitude faster than experimental quench rates (220).

In this situation, the development of fast MC equilibration algorithms for polymer melts is of great importance. An example of these techniques is the end-bridging MC move developed by Theodorou and coworkers (123, 124), which

has proven to be very efficient in equilibrating long-chain melts of chemically realistic polymer models. Mavrantzas et al. (124, 221, 222) have applied the technique to linear polyethylene melts with average chain lengths up to $N = 1000$. The method generates polydisperse systems, and in these works the authors used flat chain length distributions with polydispersity indices around $p = 1.09$. The acceptance rate for the end-bridging moves and therefore the efficiency of the algorithm depends on the degree of polydispersity allowed; these works showed that the algorithm is applicable for typical experimental polydispersities. Thus in one simulation, information for a range of chain lengths is obtained simultaneously but with reduced statistical accuracy for each chain length. Coupling the overall chain conformations to an external elongational field, represented in the simulation by a field tensor that couples to the gyration tensor of the chain and is treated as an additional thermodynamic variable defining a new simulation ensemble (223), the authors determined the elongational viscosity of the melt and the flow birefringence.

Dynamics of Chemically Realistic Models as Studied by MD Techniques

The use of MD simulation techniques to study the (dynamic) properties of polymeric materials using chemically realistic models has a long and successful history (224–226). In particular, our understanding of the conformational relaxation of polymers has profited greatly from this approach (227–229). Recently, the development of quantitatively accurate force fields (218–221) has led to the possibility of a parameter-free quantitative prediction of the relaxation behavior and transport properties of polymer melts. As already discussed, the quantum chemical determination of rotational energy barriers, which determine the relaxation behavior to a significant degree, is accurate on the electronic energy scale but still leads to non-negligible uncertainties on the thermal energy scale of the simulations.

In this situation it has proven highly successful to validate the quantum chemically determined dihedral potentials by comparison of the simulated local rotational dynamics with spin-lattice nuclear magnetic resonance (NMR) experiments (230–234). These experiments follow the reorientational motion of the CH bonds, which in turn are sensitive to the rotational barriers for dihedral angles adjacent along the chain. Different local chemical environments can be resolved and thus specific dihedral potentials can be validated. In Figure 3 we show the spin-lattice relaxation time T_1 for 12 different chemical environments in a polybutadiene melt (230) with a microstructure of 40% 1,4-*cis* units, 50% 1,4-*trans* units, and 10% 1,2-vinyl units. Establishing this kind of excellent agreement between simulation and experiment is proof that the employed force field is able to capture not only the static thermophysical properties of the specific polymer but also its transport properties. The detailed comparison between simulations and experiments performed on identical materials (microstructure, average degree of polymerization, temperature, density) yields insights into the mechanisms of molecular motion

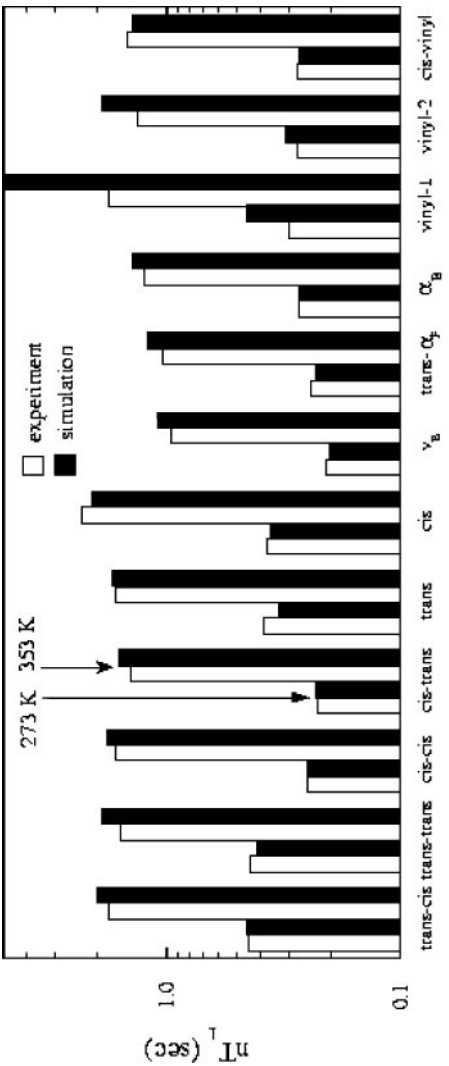

Figure 3 Spin lattice relaxation time times the number of attached hydrogen atoms for different chemical environments along a 1,4-polybutadiene chain for molecular dynamics simulations and experiment. From (230).

underlying the materials transport properties. Such models using carefully validated force fields are identical to the specific polymeric material in the range of thermodynamic parameters where they can be studied in thermal equilibrium, and they have been shown to be quantitatively predictive.

The good agreement between these models and the real material can be nicely demonstrated for instance by a comparison with neutron spin echo experiments, which analyze the chain conformational relaxation from local scales to the scale of the radius of gyration (235, 236). In Figure 4 we show a comparison between simulation and experiment for polyethylene (235) (a melt of n-C_{100} chains modeled with a chemically realistic united atom model). There is a 20% disagreement in the chain center of mass diffusion coefficient between NSE experiment and simulation (which in turn agrees with the results of a pulsed-field gradient NMR measurement) (237), and this has been absorbed into the time scaling, but the internal relaxation of the chain conformation is seen to be identical between experiment and simulation on all length scales. For the above discussed polybutadiene melt, the same level of agreement has been shown, and the high statistical accuracy of the experimental data, together with the direct measurements from simulation, allowed for the first experimental verification of the sub-diffusive center of mass motion in polymer melts for times shorter than the Rouse time (238), which had

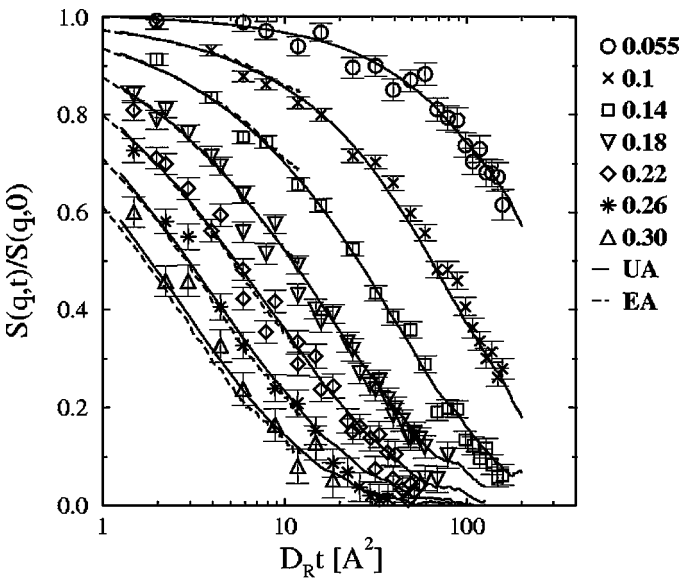

Figure 4 Comparison of the single-chain intermediate coherent dynamic structure factor in a melt of polyethylene chains of length N = 100 between experiment and simulation. The time axis is scaled by the chain center of mass diffusion coefficient. From (235).

long ago been predicted from simulations of coarse-grained models (30, 239, 240). Questions such as the range of validity of the Rouse model description of polymer melt dynamics, which for a long time had been the realm of simulations of coarse-grained models, are by now routinely analyzed using chemically realistic models (233, 234) allowing for close contact with experiment. A big remaining challenge for these types of simulations is the extension of the accessible thermodynamic parameter range, especially the extension to longer chains and lower temperatures.

Modeling Specific Polymers with Coarse-Grained Models

Computer simulations using coarse-grained models have been highly successful in furthering our understanding of the universal properties of polymers. On the other hand, the existence of a large degree of static as well as dynamic universality suggests that one can model the universal aspects of a specific polymer material using a coarse-grained model if the model can be tailored to reproduce the correct non-universal coefficients for this specific polymer. This route has been pursued by several groups over the past ten years (240–249), and the state of that research has recently been reviewed (17). The coarse-grained models are either complex lattice models such as the bond-fluctuation model (240, 242) or the 2nnd diamond lattice model (243, 244), or continuum models employing ellipsoidal repeat units (245) or standard bead-spring models (246, 247). For all these models, a suitable coarse-graining procedure of some chemically realistic polymer model (241) has to be applied first to determine the Hamiltonian for the simulation of the coarse-grained model. The conceptual basis for this approach (248) can be stated as follows: Let us denote the microscopic degrees of freedom of an atomistic model by $\{x\}$ and a set of mesoscopic degrees of freedom of this model as $\{m\}$. We can then write the canonical partition function of the atomistic model as (for notational simplicity we will use discrete states)

$$Z = \sum_x \exp\{-\beta H(x)\} = \sum_m \sum_{\{x\}_m} \exp\{-\beta H(x)\} = \sum_m \exp\{-\beta F(m)\}, \quad 31.$$

where we have defined a generalized free energy $F(m) = -k_B T \ln[\sum_{\{x\}_m} \exp(-\beta H(x)\}]$ of the mesoscopic state m. In the simplest realization of the mapping of atomistic onto coarse-grained models, the generalized free energy F would furnish an effective (temperature dependent) Hamiltonian for the simulation of the coarse-grained model. For polymers, the mesoscopic degrees of freedom, m, are mostly taken to be some coarse-grained bond lengths connecting points along the backbone of the polymer chain, which are some 5–10 carbon-carbon bonds apart, and the angles between these coarse-grained bonds. When one includes additional information on the local mobility of the polymer into the mapping (249), even a MC simulation of the bond-fluctuation model could be used to estimate the glass transition temperature of bisphenol-A-polycarbonate (240). Although the glass transition characteristics of a series of polycarbonates could be even better described using a mapping onto a bead-spring model (200, 246, 247), the physical

basis for the ability to capture dynamic properties in both of the mapping approaches, especially where it is influenced by equation of state behavior of the polymer, is still poorly understood.

Modeling Generic Polymer Systems with Coarse-Grained Models

Classical MD simulations have recently been used to study the influence of nanoparticles on the structure and dynamics of a polymer melt. By adjusting the interaction parameters between the particle and the surrounding polymer melt, one can directly identify which changes in the melt properties result from the type of interaction, and which properties change as a result of the steric hindrance introduced by the nanoparticle. In one study (250, 251), a bead-spring model for the polymers is used, in which all monomers interact via a Lennard Jones (LJ) potential. Nearest-neighbor monomers along the same chain are bound together via a FENE anharmonic spring potential. This simple polymer model has been studied in detail (18–22) and is known to be a good glass-forming system owing to the incompatibility of the preferred FENE bond distance and the LJ potential minimum.

The nanoparticle was modeled as an icosahedron, with ideal force sites at the vertices, at three equidistant sites along each edge, and at three symmetric sites on the interior of each face. The facet size was chosen roughly equal to the end-to-end distance of the surrounding polymers, in the present case roughly 10 nm. A particle was tethered to each of the force sites by a FENE spring, which maintains a relatively rigid structure but allows for thermalization of the nanoparticle. The nanoparticle sites were chosen to be more massive than the monomers, and a stiffer spring was used to minimize the oscillation of the tethered particles. Nanoparticle sites interacted with each other via a LJ potential. To determine which melt properties are a result of the steric constraints imposed by the nanoparticle and which properties are affected by polymer-nanoparticle attraction, two possible forms for the interaction between nanoparticle sites and monomers were considered: (*a*) an excluded volume interaction only and (*b*) a LJ interaction. (The excluded volume interaction was modeled by dropping the attractive r^6 term in the LJ potential.) The strength of the monomer-nanoparticle interaction was given using the Lorentz-Berthelot mixing rules. For each configuration studied, roughly 8500 particles were simulated for 10^7–10^8 time steps (of the order of 10^{11}–10^{12} atom steps). To accelerate the simulation, the rRespa multiple time-step algorithm was used (94), and the simulation was run on parallel architectures.

The nanoparticle was found to induce changes in the local melt structure (Figure 5). As in the case of polymers near a flat surface such as a wall, the density profile of the monomers has a well-defined layer structure, with the magnitude of the effect depending on the nanoparticle/polymer interaction. The changes in the density profile are accompanied by a change in the polymer conformation near the particle surface; the polymers become slightly elongated near the surface, and flatten significantly. The independence of the chain structure on

the interaction suggests that the altered shape of the polymers is primarily due to geometric constraints of packing the chains close to the surface.

The relaxation time τ of the intermediate scattering function, $F(q, t)$, which measures the decay of density fluctuations in the system and is immediately accessible to neutron scattering experiments and other techniques, can be used to quantify the effect of the nanoparticle on dynamic properties. In studies of Starr et al. (250, 251), strongly attractive nanoparticle/polymer interactions are found to slow the dynamics relative to the pure melt, whereas non-attractive interactions show an enhancement of the dynamics. From an experimental standpoint, the change in dynamics is most frequently indicated by a shift in the overall glass transition in the system. Consistent with the observations of τ, T_g of the attractive system is found to increase over that of the pure melt, while the excluded volume system exhibits a suppressed T_g. The fact that T_g shifts in opposite directions for a strongly attractive versus non-attractive nanoparticle/polymer interaction demonstrates the importance of the surface interactions in polymer/nanoparticle systems.

The self (incoherent) part $F_{\text{self}}(q, t)$ of $F(q, t)$ as a function of the monomer distance from the particle can be used to elucidate how the nanoparticle influences the local dynamics of the polymer chains (as shown in Figure 6). In the attractive system, the relaxation of the layers closest to the nanoparticle is slowest, consistent with the system dynamics being slowed by the attraction to the nanoparticle. Conversely, for the non-attractive system, the relaxation of inner layer monomers is significantly enhanced compared with the bulk, consistent with the observed enhancement of the system dynamics.

Applications of DPD and Lattice Boltzmann Techniques to Mesoscopic Phenomena

The DPD method is receiving increasing attention in the simulation of complex fluids and soft materials such as surfactants, emulsions, colloids, diblock copolymers, and polymer blends. The code is relatively simple, and it is straightforward to modify MD code to perform DPD. Accessibility to DPD code has been made easier by its inclusion in materials simulation software by Accelrys. Development of the method continues to increase its applicability to a variety of important mesoscopic phenomena in polymers for which MD and BD are inadequate given current computational speeds. Applications of DPD to polymer problems include single-chain melt dynamics (45), cross-linking of high-molecular-weight polysaccharides (48), polymer composites (49), colloid-polymer systems (50), block copolymer microphase separation (53), confined and bulk polymers in solution (54, 55), binary blend compatibility (56), viscoelastic flow (57), pressure-induced phase separation in polymer-solvent systems (58), and phase behavior of polymer solutions (59).

The field of applications of the lattice Boltzmann (LB) techniques to polymer problems is also still developing. In a recent work, Ahlrichs & Dünweg (151) studied the problem of a single chain in solution where the polymer chain is represented by a bead-spring type model and the solvent is modeled not explicitly

but by a lattice Boltzmann scheme. They showed that earlier MD results on the validity of the Zimm model for the description of polymer solution dynamics (252) could be reproduced by this new technique. In order to quantitatively match the results from the completely molecular simulation, however, solvent properties such as viscosity and especially the polymer-solvent coupling as represented by the effective monomer diffusion coefficient had to be input from earlier work. In a sense this LB application is also an example of a coarse-graining procedure from one level of modeling (molecular) to a coarser one (mixed molecular/field-theoretic). This stresses that there is, of course, a loss of information on short length and time scales in using this approach. For the larger scale properties, however, the method proved to be a factor of about 20 more efficient at the same accuracy as the earlier MD work. The relative efficiency of the method will have to be established for each application separately, but it promises to be a powerful method for the study of polymer solutions.

CONCLUSIONS

In this mini-review, we have highlighted several common methods used in simulating polymer materials on molecular and mesoscopic scales. Length restrictions prevent us from including other methods, many of which are off-shoots to those described here, and from exhaustively referencing the many outstanding simulation studies of polymer systems.

The field of polymer simulation is a growing one, in which advances in computational power, theory, and algorithms continue to enable the simulation of more and more complex problems. Although some of the methods used to model polymers are unique to soft and/or macromolecular systems, others are the same as those used to model non-polymer materials. Consequently, advances in computational materials science in general will continue to facilitate the understanding of materials and materials processing, predict properties and behavior, and predict new materials and new materials phases.

The *Annual Review of Materials Research* is online at http://matsci.annualreviews.org

LITERATURE CITED

1. Roe R, ed. 1991. *Computer Simulation of Polymers*. Englewood Cliffs, NJ: Prentice-Hall
2. Bicerano J, ed. 1992. *Computational Modeling of Polymers*. New York: Dekker
3. Colbourn E, ed. 1993. *Computer Simulation of Polymers*. Harlow, UK: Longman
4. Binder K, ed. 1995. *Monte Carlo and Molecular Dynamics Simulations in Polymer Science*. Oxford, UK: Oxford Univ. Press
5. Marx D, Hutter J. 2000. Ab initio molecular dynamics: theory and implementation. In *Modern Methods and Algorithms in Quantum Chemistry*, ed. J Grotendorst. Jülich: NIC Series
6. Ladik J. 1988. *Quantum Theory of Polymers as Solids*. New York: Plenum

7. Flory PJ. 1989. *Statistical Mechanics of Chain Molecules*. Munich: Hanser
8. DeGennes P-G. 1979. *Scaling Concepts in Polymer Physics*. Ithaca, NY: Cornell Univ. Press
9. Doi M, Edwards S. 1988. *The Theory of Polymer Dynamics*. Oxford, UK: Clarendon
10. Smith S, Hall C, Freeman B. 1995. *Phys. Rev. Lett.* 75:1316–19
11. Smith S, Hall C, Freeman B. 1996. *J. Chem. Phys.* 104:5616–37
12. Kremer K, Grest GS. 1990. *J. Chem. Phys.* 92:5057–86
13. Rudisill JW, Cummings PT. 1991. *Rheol. Acta* 30:33
14. Rudisill JW, Cummings PT. 1991. *Rheol. Acta* 30:33–43
15. Rudisill JW, Cummings PT. 1992. *J. Non-Newtonian Fluid Mech.* 41:275–88
16. Schoppe G, Heermann D. 1999. *Phys. Rev. E* 59:636–41
17. Baschnagel J, Binder K, Doruker P, Gusev AA, Hahn O, et al. 2000. In *Advances in Polymer Science: Viscoelasticity, Atomistic Models, Statistical Chemistry*, pp. 41–156. Berlin: Springer
18. Bennemann C, Donati C, Baschnagel J, Glotzer SC. 1999. *Nature* 399:246–49
19. Bennemann C, Paul W, Binder K, Dunweg B. 1998. *Phys. Rev. E* 57:843–51
20. Bennemann C, Paul W, Baschnagel J, Binder K. 1999. *J. Phys.-Conden. Matt.* 11:2179–92
21. Bennemann C, Baschnagel J, Paul W, Binder K. 1999. *Comput. Theor. Polymer Sci.* 9:217–26
22. Bennemann C, Baschnagel J, Paul W. 1999. *Eur. Phys. J. B* 10:323–34
23. Everaers R, Kremer K. 1996. *Phys. Rev. E* 53:R37–40
24. Kremer K. 1998. *Comput. Mater. Sci.* 10: 168–74
25. Escobedo FA, de Pablo JJ. 1999. *Phys. Rep.* 318:86–112
26. Micka U, Holm C, Kremer K. 1999. *Langmuir* 15:4023–44
27. Micka U, Kremer K. 2000. *Europhys. Lett.* 49:189–95
28. Shew CY, Yethiraj A. 1999. *J. Chem. Phys.* 110:5437–43
29. Verdier PH, Stockmayer WH. 1962. *J. Chem. Phys.* 36:227–35
30. Kolinski A, Skolnik J, Yaris R. 1986. *J. Chem. Phys.* 86:1567–85
31. Baumgartner A. 1992. Simulation of macromolecules. In *Monte Carlo Methods in Condensed Matter Physics*, ed. K Binder, pp. 285–316. Berlin: Springer
32. Carmesin I, Kremer K. 1988. *Macromolecules* 21:2819–23
33. Deutsch HP, Binder K. 1991. *J. Chem. Phys.* 94:2294–304
34. Wittmann HP, Kremer K, Binder K. 1990. *Comput. Phys. Commun.* 61:309–30
35. Paul W, Binder K, Heermann DW, Kremer K. 1991. *J. Phys. II* 1:37–60
36. Deutsch HP, Binder K. 1992. *Europhys. Lett.* 17:697–702
37. Dickmann R. 1987. *J. Chem. Phys.* 87: 2246–48
38. Müller M. 1999. *Macromol. Theory Simul.* 8:343–74
39. Muller M, Schmid F. 1999. Monte Carlo simulation of interfaces in polymer blends. In *Annual Reviews of Computational Physics*, ed. D Stauffer, pp. 59–127. Singapore: World Scientific
40. Ivanov VA, Paul W, Binder K. 1998. *J. Chem. Phys.* 109:5659–69
41. Kreitmeier S, Wittkop M, Göritz D. 1999. *Phys. Rev. E* 59:1982–88
42. Panagiotopoulos AZ, Kumar SK. 1999. *Phys. Rev. Lett.* 83:2981–84
43. Panagiotopoulos AZ. 2000. *J. Chem. Phys.* 112:7132–37
44. Hoogerbrugge PJ, Koelman JMVA. 1992. *Europhys. Lett.* 19:155–60
45. Akkermans RLC, Briels WJ. 2000. *J. Chem. Phys.* 113:6409–22
46. Avalos JB, Mackie AD. 1999. *J. Chem. Phys.* 111:5267–76
47. Ball RC, Melrose JR. 1997. *Physica A* 247:444–72

48. Coveney PV, De Silva H, Gomtsyan A, Whiting A, Boek ES. 2000. *Mol. Simul.* 25:265
49. Elliott JA, Windle AH. 2000. *J. Chem. Phys.* 113:10367–76
50. Gibson JB, Zhang K, Chen K, Chynoweth S, Manke CW. 1999. *Mol. Simul.* 23:1–41
51. Gibson JB, Chen K. 1999. *Int. J. Mod. Phys. C* 10:241–61
52. Groot RD, Warren PB. 1997. *J. Chem. Phys.* 107:4423–35
53. Groot RD, Madden TJ, Tildesley DJ. 1999. *J. Chem. Phys.* 110:9739–49
54. Kong Y, Manke CW, Madden WG, Schlijper AG. 1994. *Int. J. Thermophys.* 15:1093–101
55. Schlijper AG, Hoogerbrugge PJ, Manke CW. 1995. *J. Rheol.* 39:567–79
56. Spyriouni T, Vergelati C. 2001. *Macromolecules* 34:5306–16
57. ten Bosch BIM. 1999. *J. Non-Newtonian Fluid Mech.* 83:231–48
58. van Vliet RE, Hoefsloot HCJ, Hamersma PJ, Iedema PD. 2000. *Macromol. Theor. Simul.* 9:698–702
59. Wijmans CM, Smit B, Groot RD. 2001. *J. Chem. Phys.* 114:7644–54
60. Willemsen SM, Vlugt TJH, Hoefsloot HCJ, Smit B. 1998. *J. Comput. Phys.* 147:507–17
61. Willemsen SM, Hoefsloot HCJ, Iedema PD. 2000. *Int. J. Mod. Phys. C* 11:881–90
62. Gibson JB, Chen K, Chynoweth S. 1998. *J. Colloid Interface Sci.* 206:464–74
63. Dzwinel W, Yuen DA. 2000. *J. Colloid Interface Sci.* 225:179–90
64. Dzwinel W, Yuen DA. 2000. *Int. J. Mod. Phys. C* 11:1–25
65. Glotzer SC. 1995. Computer simulations of spinodal decomposition in polymer blends. In *Annual Reviews of Computational Physics*, ed. D Stauffer, pp. 1–46. Singapore: World Scientific
66. Fraaije JGEM. 1993. *J. Chem. Phys.* 99: 9202–12
67. Fraaije JGEM. 1994. *J. Chem. Phys.* 100: 6984
68. Fraaije JGEM, Evers OA. 1995. Implementation of dynamic density functional theory for self-organizing complex fluids on parallel computers. In *High-Performance Computing and Networking*, pp. 441–47. Berlin: Springer
69. Fraaije JGEM, vanVlimmeren BAC, Maurits NM, Postma M, Evers OA, et al. 1997. *J. Chem. Phys.* 106:4260–69
70. Maurits NM, Fraaije JGEM. 1997. *J. Chem. Phys.* 106:6730–43
71. Kawakatsu T, Doi M, Hasegawa R. 1999. *Int. J. Mod. Phys. C* 10:1531–40
72. Morita H, Kawakatsu T, Doi M. 1999. *Kobunshi Ronbunshu* 56:674–83
73. Morita H, Kawakatsu T, Doi M. 2001. *Macromolecules* 34:8777–83
74. Ganesan V, Fredrickson GH. 2001. *Europhys. Lett.* 55:814–20
75. Fredrickson GH, Ganesan V, Drolet F. 2002. *Macromolecules* 35:16–39
76. Bird RB, Armstrong RC, Hassager O. 1987. *Dynamics of Polymeric Liquids*. New York: Wiley
77. Larson RG. 2000. *Structure and Dynamics of Complex Fluids.* Oxford, UK: Oxford Univ. Press
78. Cormenzana J, Ledda A, Laso M, Debbaut B. 2001. *J. Rheol.* 45:237–58
79. Feigl L, Laso M, Öttinger HC. 1995. *Macromolecules* 28:3261–74
80. Gusev AA. 1997. *J. Mech. Phys. Solids* 45:1449
81. Glotzer SC, Starr FW. 2001. Towards multiscale simulation of filled and nanofilled polymers. In *Foundations of Molecular Modeling and Simulation, AlChE Symp. Ser.*, ed. PT Cummings, P Westmoreland, B Carnahan, 97:44–53
82. Starr FW, Glotzer SC. 2001. *Molecular and Mesoscale Simulations of Filled and Nanofilled Polymers*. Mater. Res. Soc. Symp. Series 661, p. 1
83. Car R, Parrinello M. 1985. *Phys. Rev. Lett.* 55:2471–74
84. Grotendorst J, ed. 2000. *Modern Methods and Algorithms in Quantum Chemistry*. Julich, Germany: NIC Series

85. Parr RG, Yang W. 1989. *Density Functional Theory of Atoms and Molecules*. Oxford, UK: Oxford Univ. Press
86. Tuckerman ME, Hughes A. 1998. Path integral molecular dynamics: a computational approach to quantum statistical mechanics. In *Quantum and Classical Dynamics in Condensed Phase Simulations*, ed. BJ Berne, G Ciccotti, DF Coker. Singapore: World Scientific
87. Berne BJ, Ciccotti G, Coker DF, eds. 1998. *Quantum and Classical Dynamics in Condensed Phase Simulations*. Singapore: World Scientific
88. Binder K, Ciccotti G, eds. 1996. *Monte Carlo and Molecular Dynamics Simulations of Condensed Matter Systems*. Bologna, Italy: Soc. Italiana di Fisica
89. Allen MP, Tildesley DJ. 1993. *Computer Simulation of Liquids*. New York: Oxford Univ. Press
90. Frenkel D, Smit B. 1996. *Understanding Molecular Simulation: From Algorithms to Applications*. San Diego: Academic
91. Rappaport DC. 1995. *The Art of Molecular Dynamics Simulation*. Cambridge, UK: Cambridge Univ. Press
92. Sarman SS, Evans DJ, Cummings PT. 1998. *Phys. Rep.* 305:1–92
93. Duan Y, Kollman PA. 1998. *Science* 282: 740–44
94. Tuckerman M, Berne BJ, Martyna GJ. 1992. *J. Chem. Phys.* 97:1990–2001
95. Ermak DL, McCammon JA. 1978. *J. Chem. Phys.* 69:1352
96. Liu TW. 1989. *J. Chem. Phys.* 90:5826
97. Zylka W, Öttinger HC. 1989. *J. Chem. Phys.* 90:474
98. Grassia P, Hinch EJF. 1996. *J. Fluid Mech.* 308:255
99. Doyle PS, Shaqfeh ESG, Gast AP. 1997. *J. Fluid Mech.* 334:251
100. Öttinger HC. 1996. *Stochastic Processes in Polymeric Fluids*. New York: Springer
101. Español P, Warren PB. 1995. *Europhys. Lett.* 30:191
102. Marsh CA, Yeomans JM. 1997. *Europhys. Lett.* 37:511
103. Martys NS, Mountain RD. 1999. *Phys. Rev. E* 59:3733–36
104. Binder K, ed. 1992. *Monte Carlo Methods in Condensed Matter Physics*. Berlin: Springer-Verlag
105. Binder K, ed. 1984. *Applications of the Monte Carlo Method in Statistical Physics*. Berlin: Springer-Verlag
106. Khalatur PG, Shirvanyanz DG, Starovoitova NY, Khokhlov AR. 2000. *Macromol. Theory Simul.* 9:141–55
107. Binder K, Paul W. 1997. *J. Polym. Sci. Polym. Phys.* 35:1–37
108. Sokal AD. 1995. Monte Carlo methods for the self-avoiding walk. In *Monte Carlo and Molecular Dynamics Methods in Polymer Science*, ed. K Binder, pp. 47–127. Oxford, UK: Oxford Univ. Press
109. Kron AK. 1965. *Polym. Sci. USSR* 7: 1361–67
110. Harris J, Rice SA. 1988. *J. Chem. Phys.* 88:1298–306
111. Wall FT, Mandel F. 1975. *J. Chem. Phys.* 63:4592–95
112. Siepmann JI, Frenkel D. 1992. *Molec. Phys.* 75:59–70
113. de Pablo JJ, Laso M, Suter UW. 1992. *J. Chem. Phys.* 96:2395–403
114. Escobedo FA, de Pablo JJ. 1997. *J. Chem. Phys.* 106:793–810
115. Escobedo FA, de Pablo JJ. 1995. *J. Chem. Phys.* 102:2636–52
116. Frenkel D. 1995. Numerical techniques to study complex liquids. In *Observation, Prediction and Simulation of Phase Transitions in Complex Fluids*, ed. M Baus, LF Rull, J-P Ryckaert, pp. 357–419. Netherlands: Kluwer
117. Lal M. 1969. *Mol. Phys.* 17:57–64
118. MacDonald B, Jan N, Hunter DL, Steinitz MO. 1985. *J. Phys. A* 18:2627–31
119. Madras N, Sokal AD. 1988. *J. Stat. Phys.* 50:109–86
120. Leontidis E, de Pablo JJ, Laso M, Suter UW. 1994. *Adv. Polym. Sci.* 116:283–318
121. Dodd LR, Boone TD, Theodorou DN. 1993. *Mol. Phys.* 78:961–96

122. Santos S, Suter AW, Mueller M, Nievergelt J. 2001. *J. Chem. Phys.* 114:9772–79
123. Pant PVK, Theodorou DN. 1995. *Macromolecules* 28:7224–34
124. Mavrantzas VG, Boone TD, Zervopoulou E, Theodorou DN. 1999. *Macromolecules* 32:5072–96
125. Kofke DA. 1999. Semi-grand canonical Monte Carlo simulations: integration along coexistence lines. In *Monte Carlo Methods in Chemical Physics*, ed. DM Ferguson, JI Siepmann, DG Truhlar, pp. 405–41. New York: Wiley
126. Kofke DA, Glandt ED. 1987. *J. Chem. Phys.* 87:4881–90
127. Sariban A, Binder K. 1987. *J. Chem. Phys.* 86:5859–73
128. Sariban A, Binder K. 1988. *Colloid Polym. Sci.* 267:469–79
129. Müller M, Binder K. 1998. *Macromolecules* 31:8323–46
130. Panagiotopoulos AZ, Quirke N, Stapleton M, Tildesley DJ. 1988. *Mol. Phys.* 63:527–45
131. Panagiotopoulos AZ. 1987. *Mol. Phys.* 61:813–26
132. Smit B, De Smedt PH, Frenkel D. 1989. *Mol. Phys.* 68:931–50
133. Mitsutake A, Sugita Y, Okamoto Y. 2001. *Biopolymers* 60:96–123
134. Yan QL, de Pablo JJ. 2000. *J. Chem. Phys.* 113:1276–82
135. Yan QL, de Pablo JJ. 1999. *J. Chem. Phys.* 111:9509–16
136. Müller M, Paul W. 1994. *J. Chem. Phys.* 100:719–24
137. Wilding NB, Müller M. 1994. *J. Chem. Phys.* 101:4324–30
138. Paul W, Müller M. 2001. *J. Chem. Phys.* 115:630–35
139. Bunker A, Dünweg B. 2001. *Phys. Rev. E* 63
140. Grassberger P. 1997. *Phys. Rev. E* 56: 3682–93
141. Chen S, Doolen GD. 1998. *Annu. Rev. Fluid Mech.* 30:329–64
142. Benzi R, Succi S, Vergassola M. 1992. *Phys. Rep.* 222:145–97
143. Malevanets A, Yeomans JM. 1999. *Faraday Discus.* 112:237–48
144. Gonnella G, Orlandini E, Yeomans JM. 1998. *Nuovo Cimento D* 20:2393–99
145. Wagner AJ, Yeomans JM. 1998. *Int. J. Mod. Phys. C* 9:1373–82
146. Gonnella G, Orlandini E, Yeomans JM. 1999. *Phys. Rev. E* 59:R4741–44
147. Wagner AJ, Yeomans JM. 1999. *Phys. Rev. E* 59:4366–73
148. Gonnella G, Orlandini E, Yeomans JM. 1997. *Int. J. Mod. Phys. C* 8:783–92
149. Orlandini E, Gonnella G, Yeomans JM. 1997. *Physica A* 240:277–85
150. Gonnella G, Orlandini E, Yeomans JM. 1997. *Phys. Rev. Lett.* 78:1695–98
151. Ahlrichs P, Dünweg B. 1999. *J. Chem. Phys.* 111:8225–39
152. Denniston C, Orlandini E, Yeomans JM. 2000. *Europhys. Lett.* 52:481–87
153. Denniston C, Orlandini E, Yeomans JM. 2001. *Phys. Rev. E* 64:021701:1–11
154. Cahn JW. 1959. *J. Chem. Phys.* 30:1121–24
155. Cahn JW. 1961. *Acta Metall.* 9:795–801
156. Cahn JW, Hilliard JE. 1971. *Acta Metall.* 19:151–61
157. Wiltzius P, Bates FS, Heffner W. 1988. *Phys. Rev. Lett.* 60:1538
158. Zhang ZL, Zhang HD, Yang YL. 2000. *J. Chem. Phys.* 113:8348–61
159. Zhang ZL, Zhang HD, Yang YL, Vinckier I, Laun HM. 2001. *Macromolecules* 34:1416–29
160. Cao Y, Zhang HD, Xiong Z, Yang YL. 2001. *Macromol. Theor. Simul.* 10:314–24
161. Sun T, Balazs AC, Jasnow D. 1999. *Phys. Rev. E* 59:603–11
162. Sun T, Balazs AC, Jasnow D. 1997. *Phys. Rev. E* 55:R6344–47
163. Oono Y, Puri S. 1987. *Phys. Rev. Lett.* 58: 836–39
164. Oono Y, Puri S. 1988. *Phys. Rev. A* 38: 434–53
165. Puri S, Oono Y. 1988. *Phys. Rev. A* 38: 1542–65

166. Oono Y, Puri S, Yeung C, Bahiana M. 1988. *J. Appl. Crystall.* 21:883–85
167. Altevogt P, Evers OA, Fraaije JGEM, Maurits NM, van Vlimmeren BAC. 1999. *J. Mol. Struct. Theochem.* 463:139–43
168. Fraaije JGEM, Zvelindovsky AV, Sevink GJA, Maurits NM. 2000. *Mol. Simul.* 25:131–44
169. Maurits NM, Fraaije JGEM. 1997. *J. Chem. Phys.* 107:5879–89
170. Maurits NM, vanVlimmeren BAC, Fraaije JGEM. 1997. *Phys. Rev. E* 56:816–25
171. Maurits NM, Zvelindovsky AV, Fraaije JGEM. 1998. *J. Chem. Phys.* 109: 11032–42
172. Maurits NM, Zvelindovsky AV, Sevink GJA, van Vlimmeren BAC, Fraaije JGEM. 1998. *J. Chem. Phys.* 108:9150–54
173. Maurits NM, Zvelindovsky AV, Fraaije JGEM. 1998. *J. Chem. Phys.* 108:2638–50
174. Maurits NM, Sevink GJA, Zvelindovsky AV, Fraaije JGEM. 1999. *Macromolecules* 32:7674–81
175. Morozov AN, Fraaije JGEM. 2001. *J. Chem. Phys.* 114:2452–65
176. Sevink GJA, Zvelindovsky AV, van Vlimmeren BAC, Maurits NM, Fraaije JGEM. 1999. *J. Chem. Phys.* 110:2250–56
177. Sevink A, Zvelindovsky A, Fraaije JGEM. 2000. *Prog. Theor. Phys. Suppl.* 138:320–29
178. Sevink GJA, Zvelindovsky AV, Fraaije JGEM, Huinink HP. 2001. *J. Chem. Phys.* 115:8226–30
179. van Vlimmeren BAC, Maurits NM, Zvelindovsky AV, Sevink GJA, Fraaije JGEM. 1999. *Macromolecules* 32:646–56
180. Zvelindovsky AVM, van Vlimmeren BAC, Sevink GJA, Maurits NM, Fraaije JGEM. 1998. *J. Chem. Phys.* 109:8751–54
181. Zvelindovsky AV, Sevink GJA, van Vlimmeren BAC, Maurits NM, Fraaije JGEM. 1998. *Phys. Rev. E* 57:R4879–82
182. Zvelindovsky AV, Sevink GJA, Fraaije JGEM. 2000. *Phys. Rev. E* 62:R3063–66
183. Lee BP, Douglas JF, Glotzer SC. 1999. *Phys. Rev. E* 60:5812–22
184. Balazs AC, Ginzburg VV, Qiu F, Peng GW, Jasnow D. 2000. *J. Phys. Chem. B* 104:3411–22
185. Ginzburg VV, Peng G, Qiu F, Jasnow D, Balazs AC. 1999. *Phys. Rev. E* 60:4352–59
186. Ginzburg VV, Qiu F, Paniconi M, Peng GW, Jasnow D, Balazs AC. 1999. *Phys. Rev. Lett.* 82:4026–29
187. Ginzburg VV, Gibbons C, Qiu F, Peng GW, Balazs AC. 2000. *Macromolecules* 33:6140–47
188. Ginzburg VV, Qiu F, Balazs AC. 2002. *Polymer* 43:461–66
189. Peng GW, Qiu F, Ginzburg VV, Jasnow D, Balazs AC. 2000. *Science* 288:1802–4
190. Qiu F, Ginzburg VV, Paniconi M, Peng GW, Jasnow D, Balazs AC. 1999. *Langmuir* 15:4952–56
191. Qiu F, Peng GW, Ginzburg VV, Balazs AC, Chen HY, Jasnow D. 2001. *J. Chem. Phys.* 115:3779–84
192. Glotzer SC, Coniglio A. 1994. *Phys. Rev. E* 50:4241–44
193. Glotzer SC, Dimarzio EA, Muthukumar M. 1994. *Abstr. Pap. Am. Chem. Soc.* 208:350–PMS0
194. Glotzer SC, Stauffer D, Jan N. 1994. *Phys. Rev. Lett.* 72:4109–12
195. Glotzer SC, Dimarzio EA, Muthukumar M. 1995. *Phys. Rev. Lett.* 74:2034–37
196. Glotzer SC, Stauffer D, Jan N. 1995. *Phys. Rev. Lett.* 75:1675–76
197. Drolet F, Fredrickson GH. 2001. *Macromolecules* 34:5317–24
198. Deleted in proof
199. Abraham FF, Broughton JQ, Bernstein N, Kaxiras E. 1998. *Comput. Phys.* 12:538
200. Kremer K, Muller-Plathe F. 2001. *Mater Res. Soc. Bull.* 26:205–10
201. Boero M, Parrinello M, Weiss H, Hüffer S. 2001. *J. Phys. Chem. A* 105:5096–105
202. Martonak R, Paul W, Binder K. 1997. *J. Chem. Phys.* 106:8918–30
203. Sorensen R, Liau WB, Kesner L, Boyd RH. 1988. *Macromolecules* 21:200–8

204. Rutledge GC, Lacks DJ, Martonak R, Binder K. 1998. *J. Chem. Phys.* 108: 10274–80
205. Kreitmeier SN, Liang GL, Noid DW, Wunderlich B. 1995. *J. Chem. Soc. Faraday Trans.* 91:2601–8
206. Smith GD, Paul W. 1998. *J. Phys. Chem. A* 102:1200–8
207. Schatz GC. 1989. *Rev. Mod. Phys.* 61: 669–88
208. Dasgupta S, Hammond WB, Goddard WA. 1996. *J. Am. Chem. Soc.* 118:12291–301
209. Smith GD, Jaffe RL. 1996. *J. Phys. Chem. A* 100:18718–24
210. Smith GD, Borodin O, Bedrov D. 1998. *J. Phys. Chem. A* 102:10318–23
211. Qiu XH, Ediger MD. 2000. *Macromolecules* 33:490–98
212. Siepmann JI, Karaborni S, Smit B. 1993. *Nature* 365:330–32
213. Smit B, Karaborni S, Siepmann JI. 1995. *J. Chem. Phys.* 102:2126–40
214. Laso M, de Pablo JJ, Suter UW. 1992. *J. Chem. Phys.* 97:2817–19
215. Poncela A, Rubio AM, Freire JJ. 2001. *J. Chem. Phys.* 114:8174–80
216. Wilding NB, Müller M, Binder K. 1996. *J. Chem. Phys.* 105:802–9
217. Kumar S, Weinhold JD. 1996. *Phys. Rev. Lett.* 77:1512–15
218. Brown D, Clarke JHR, Okuda M, Yamazaki T. 1994. *J. Chem. Phys.* 100:6011–18
219. Baschnagel J. 1995. *Phys. Rev. B* 49:135–46
220. Han J, Gee RH, Boyd RH. 1994. *Macromolecules* 27:7781–84
221. Mavrantzas VG, Theodorou DN. 2000. *Comp. Theor. Polym. Sci.* 10:1–13
222. Mavrantzas VG, Theodorou DN. 2000. *Macromol. Theory Simul.* 9:500–15
223. Mavrantzas V, Theodorou DN. 1998. *Macromolecules* 31:6310–32
224. Rigby D, Roe RJ. 1991. Local chain motion studied by molecular dynamics simulation of polymer liquid and glass. In *Computer Simulation of Polymers*, ed. R Roe, pp. 79–93. Englewood Cliffs, NJ: Prentice-Hall
225. Ryckaert JP, McDonald IR, Klein ML. 1991. Use of an all-atom semiflexible model in molecular dynamic simulation of long-chain paraffins. In *Computer Simulation of Polymers*, ed. RJ Roe. Englewood Cliffs, NJ: Prentice-Hall
226. Clarke JHR. 1995. Molecular dynamics of glassy polymers. In *Monte Carlo and Molecular Dynamics Simulations in Polymer Science*, ed. K Binder, pp. 272–306. Oxford, UK: Oxford Univ. Press
227. Helfand E, Wasserman ZR, Weber TA. 1980. *Macromolecules* 13:526–33
228. Gee R, Boyd RH. 1998. *Comput. Theor. Polym. Sci.* 8:93–98
229. Gee R, Boyd RH. 1994. *J. Chem. Phys.* 101:8028–38
230. Smith G, Borodin O, Bedrov D, Paul W, Qiu X, Ediger M. 2001. *Macromolecules* 34:5192–99
231. Smith G, Yoon DY, Zhu W, Ediger M. 1994. *Macromolecules* 28:5563–69
232. Smith G, Yoon DY, Wade CG, OLeary D, Chen A, Jaffe RL. 1997. *J. Chem. Phys.* 106:3798–805
233. Paul W, Smith GD, Yoon DY. 1997. *Macromolecules* 30:7772–80
234. Mondello M, Grest GS, Garcia AR, Silbernagel BG. 1996. *J. Chem. Phys.* 105:5208–15
235. Paul W, Smith GD, Yoon DY, Farago B, Rathgeber S, et al. 1998. *Phys. Rev. Lett.* 80:2346–49
236. Smith GD, Paul W, Monkenbusch M, Richter D. 2001. *J. Chem. Phys.* 114: 4285–88
237. Pearson D, Fetters LJ, Graessley WW, Ver Strate G, von Meerwall E. 1994. *Macromolecules* 27:711–19
238. Smith GD, Paul W, Monkenbusch M, Richter D. 2000. *Chem. Phys.* 261:61–74
239. Kolinski A, Skolnik J, Yaris R. 1986. *J. Chem. Phys.* 86:7164–73
240. Paul W, Binder K, Kremer K, Heermann D. 1991. *Macromolecules* 24:6332–34

241. Baschnagel J, Binder K, Paul W, Laso M, Suter UW, et al. 1991. *J. Chem. Phys.* 95: 6014–25
242. Tries V, Paul W, Baschnagel J, Binder K. 1997. *J. Chem. Phys.* 106:738–48
243. Rapold RF, Mattice WL. 1995. *J. Chem. Soc. Faraday Trans.* 91:2435–41
244. Doruker P, Mattice WL. 1997. *Macromolecules* 30:5520–26
245. Zimmer K, Linke A, Heermann DW, Batoulis J, Bürger T. 1996. *Macromol. Theor. Simul.* 5:1065–74
246. Tschop W, Kremer K, Batoulis J, Burger T, Hahn O. 1998. *Acta Polym.* 49:61–74
247. Tschop W, Kremer K, Hahn O, Batoulis J, Burger T. 1998. *Acta Polym.* 49:75–79
248. Paul W. 2001. A mapping from atomistic polymer models to coarse-grained models. In *Multiscale Computational Methods in Chemistry and Physics*, ed. A Brandt, J Bernholc, K Binder, pp. 285–87. Amsterdam: IOS Press
249. Paul W, Pistoor N. 1994. *Macromolecules* 27:1249–55
250. Starr FW, Schroeder TB, Glotzer SC. 2001. *Phys. Rev. E* 62:021802:1–5
251. Starr FW, Schroeder TB, Glotzer SC. 2001. *Macromolecules.* In press
252. Dünweg B, Kremer K. 1993. *J. Chem. Phys.* 99:6983–97

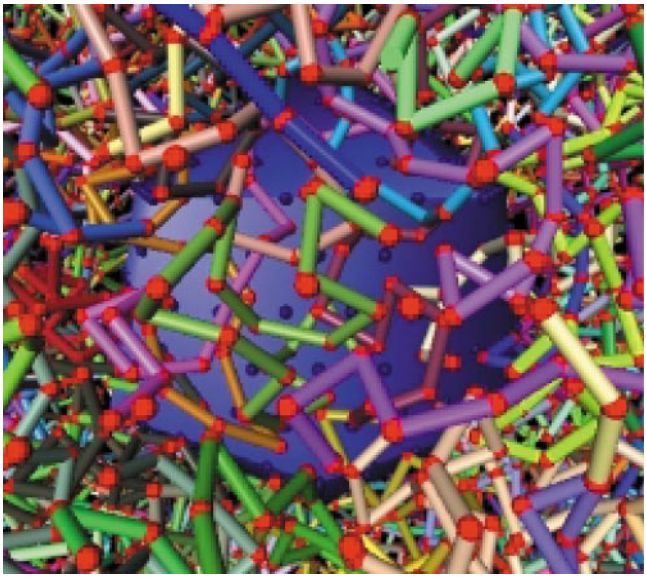

Figure 5 Model of a nanoparticle embedded in dense polymer melt (image shown represents only a portion of the total simulation box, which contains 400 chains of 20 monomers each in addition to the nanoparticle). From F.W. Starr and S.C. Glotzer.

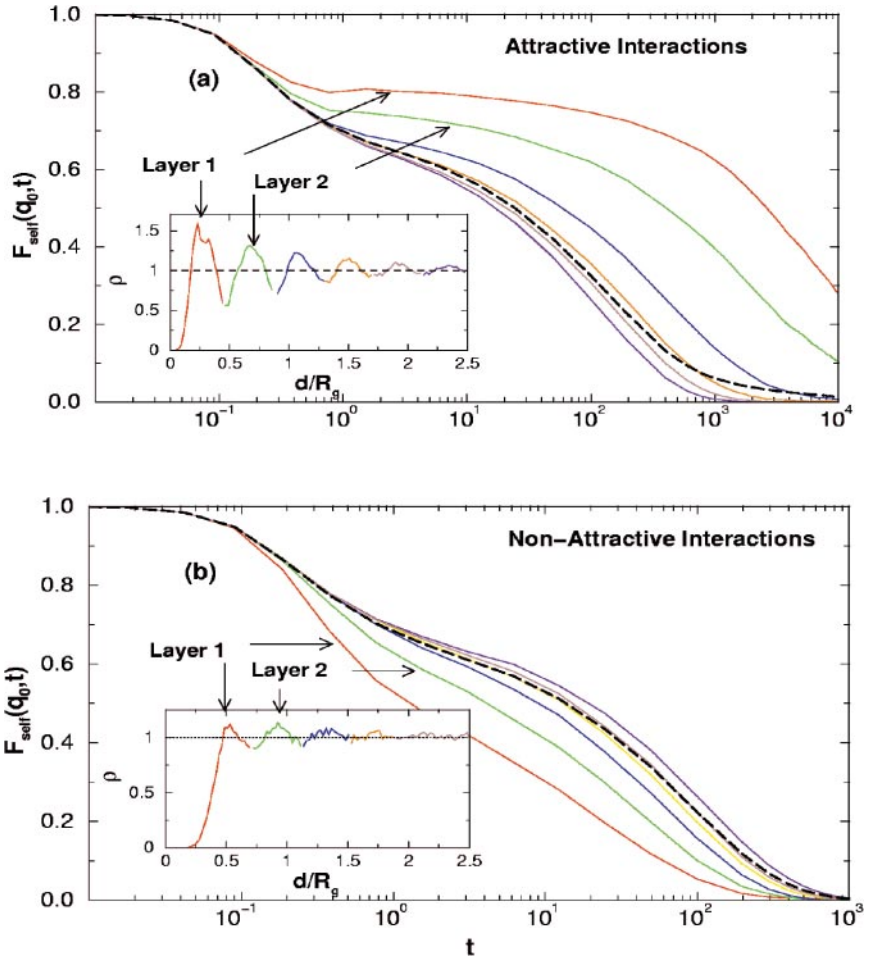

Figure 6 Relaxation of the self part of the intermediate scattering function decomposed into the contribution of each layer of polymer around the nanoparticle (indicated in the insets). The surface polymers exhibit the slowest dynamics in the case of the attractive nanoparticle (*top figure*), whereas they exhibit the fastest dynamics in the case of the non-attractive nanoparticle (*bottom figure*). From F.W. Starr, T.B. Schrøder & S.C. Glotzer.